AFGL-TR-86-0028
ENVIRONMENTAL RESEARCH PAPERS, NO. 946

Improving foF2 Prediction for the Sunrise Transition Period

B.S. DANDEKAR
J. BUCHAU

29 January 1986

IONOSPHERIC PHYSICS DIVISION
PROJECT 4643
AIR FORCE GEOPHYSICS LABORATORY
HANSCOM AFB, MA 01731

"This technical report has been reviewed and is approved for publication."

FOR THE COMMANDER

WILLIAM K. VICKERY
Acting Branch Chief

ROBERT A. SKRIVANEK
Division Director

This document has been reviewed by the ESD Public Affairs Office (PA) and is releasable to the National Technical Information Service (NTIS).

Qualified requestors may obtain additional copies from the Defense Technical Information Center. All others should apply to the National Technical Information Service.

If your address has changed, or if you wish to be removed from the mailing list, or if the addressee is no longer employed by your organization, please notify AFGL/DAA, Hanscom AFB, MA 01731. This will assist us in maintaining a current mailing list.

ADA 170451

Unclassified

SECURITY CLASSIFICATION OF THIS PAGE

REPORT DOCUMENTATION PAGE

1a. REPORT SECURITY CLASSIFICATION: Unclassified	1b. RESTRICTIVE MARKINGS
2a. SECURITY CLASSIFICATION AUTHORITY	3. DISTRIBUTION/AVAILABILITY OF REPORT: Approved for public release; distribution unlimited
2b. DECLASSIFICATION/DOWNGRADING SCHEDULE	
4. PERFORMING ORGANIZATION REPORT NUMBER(S): AFGL-TR-86-0028 ERP, No. 946	5. MONITORING ORGANIZATION REPORT NUMBER(S)
6a. NAME OF PERFORMING ORGANIZATION: Air Force Geophysics Laboratory; 6b. OFFICE SYMBOL (If applicable): LIS	7a. NAME OF MONITORING ORGANIZATION
6c. ADDRESS (City, State and ZIP Code): Hanscom AFB, Massachusetts 01731	7b. ADDRESS (City, State and ZIP Code)
8a. NAME OF FUNDING/SPONSORING ORGANIZATION; 8b. OFFICE SYMBOL (If applicable)	9. PROCUREMENT INSTRUMENT IDENTIFICATION NUMBER
8c. ADDRESS (City, State and ZIP Code)	10. SOURCE OF FUNDING NOS.

PROGRAM ELEMENT NO.	PROJECT NO	TASK NO.	WORK UNIT NO
62101F	4643	08	03

11. TITLE (Include Security Classification): Improving foF2 Prediction for the (contd.)	
12. PERSONAL AUTHOR(S): Dandekar, B.S., and Buchau, J.	
13a. TYPE OF REPORT: Scientific Final; 13b. TIME COVERED: FROM 10/84 TO 9/85	14. DATE OF REPORT (Yr., Mo., Day): 1986 January 29; 15. PAGE COUNT: 64
16. SUPPLEMENTARY NOTATION	

17. COSATI CODES		
FIELD	GROUP	SUB GR
04	01	

18. SUBJECT TERMS (Continue on reverse if necessary and identify by block number)

Ionospheric prediction
Ionospheric modeling
Ionospheric parameters
OTH frequency management

19. ABSTRACT (Continue on reverse if necessary and identify by block number)

During the 2- to 3-hr sunrise transition period, the relative change in foF2 is 20-60 percent per hour and is independent of solar activity. The change is largest in winter and smallest in summer. To prevent the skip distance from changing by more than 250 km, that is, to maintain continuous illumination of at least 50 percent of the barrier (nominal width 500 km), requires that the operating frequency be changed for every 6 percent change in foF2. Thus, in the case of an OTH system, the operating frequency has to be adjusted during the sunrise period every 6 to 20 min (seasonal dependence) for satisfactory performance. To accommodate such rapid changes, an empirical algorithm has been tested for improved foF2 predictions during sunrise. The prediction scheme is based on the availability of relevant (under the oblique raypath) real time ionospheric data. Using the average hourly gradient obtained from the previous four days' foF2 observations and the "now" value, the foF2 for the next hour is predicted. A further improvement is achieved, if a correction is added, which modifies the average slope depending on the current (cont.)

20. DISTRIBUTION/AVAILABILITY OF ABSTRACT: UNCLASSIFIED/UNLIMITED ☒ SAME AS RPT ☐ DTIC USERS ☐	21. ABSTRACT SECURITY CLASSIFICATION: Unclassified

22a. NAME OF RESPONSIBLE INDIVIDUAL	22b. TELEPHONE NUMBER (Include Area Code)	22c. OFFICE SYMBOL
B.S. Dandekar	(617) 377-3122	AFGL/LIS

DD FORM 1473, 83 APR EDITION OF 1 JAN 73 IS OBSOLETE

Unclassified

SECURITY CLASSIFICATION OF THIS PAGE

Block 11 (cont.).

Sunrise Transition Period

Block 19 (cont.).

foF2 being larger or smaller than the mean of the past four days for the respective hour. This new prediction scheme makes the prediction independent of a predicted sunspot number and reduces the prediction error (ΔfoF2) by 0.4, 0.7, and 1.7 MHz at levels of median, $\pm\sigma$, and the extremes distribution of foF2 of populations (or 86, 47, and 26 percent respectively), as compared with the use of a straight IONCAP model prediction, which requires a prediction of the expected sunspot number. In case of (temporary) lack of either past or real time data, the prediction scheme allows the use of IONCAP to accomplish a degraded prediction. The proposed method yields predictions better than the best that IONCAP could produce even if the smoothed monthly sunspot number could be predicted correctly.

Contents

Illustrations

Illustrations

Tables

Tables

Improving foF2 Prediction for the Sunrise Transition period

1. INTRODUCTION

During the transition period of sunrise (and sunset), the critical frequency foF2 of the ionospheric F-layer changes at a rapid rate, demanding more frequent changes in the operating frequency of an OTH-B radar to maintain a relatively constant barrier location. The observations as well as predictions from ionospheric models show that the change in foF2 is between 20 and 60 percent (average 30 percent) per hour during the sunrise period (05-09 LT) from October through March independent of the phase of the solar activity cycle.

An OTH-B surveillance radar is required to maintain a barrier at a distance of 2000 km from the radar. During regular daytime and nighttime operations, when the ionosphere is in general a horizontally stratified medium, a backscatter system can illuminate a large area beyond the skip distance. During sunrise hours, however, the sunrise-related tilt of the F-layer results in a narrowing of the backscatter radar "footprint," that is, the useful range for target detection. In this discussion, we consider a nominal value of 500 km (275 nm) as the morning hour useful barrier width. In order to track targets crossing this narrow barrier, it is considered important that the radar footprints before and after an operational frequency change overlap by approximately 50 percent or 250 km. This will ensure

(Received for publication 22 January 1986)

that about 50 percent of the already established targets will be illuminated after the frequency switch, providing track continuity important to the identification process during times when aircraft on the average cross the barrier in approximately 35 minutes.

Therefore, during the sunrise period, the frequency would have to be changed every time the barrier moves towards the radar by 250 km. At a distance of 2250 km from the transmitter, that is, in the center of a nominal barrier extending from 2000 km to 2500 km, the M-factor (which relates the radar operation frequency to foF2 at the reflection point) changes at a rate of 2.3 percent for every 100 km. Conversely, this means that, for every 2.3 percent change in M-factor (and therefore in foF2), the barrier will move 100 km towards the radar during sunrise. Therefore, for every 5.8 percent change in M-factor or foF2, the barrier will shift the maximum permissible 250 km. To keep up with a 30 percent per hour change in foF2 during sunrise hours, and maintain a 50 percent overlap of the barrier through each frequency change, the operating frequency of the radar has to be adjusted at least 5 times per hour. It is therefore desirable to have reliable short term predictions of foF2 for the coverage region of interest, to facilitate the necessary rapid changes in operating frequency.

Inspection of three readily available techniques showed that they would not solve the problem. These techniques are: the use of existing models, the extrapolation of foF2 from measurements at a different location (such as the radar site), and extrapolation of the expected sunrise transition from the foF2 sunrise transition measured earlier at a more easterly location. The ITS-78[1] or IONCAP[2] monthly median prediction models (Lloyd et al[2]) yield an foF2 prediction error of ± 1.5 MHz. These models are unable to provide the required accuracy of $\leqslant 0.5$ MHz needed by the real time operational systems (this requirement for sunrise transition will be substantiated in Section 2). Rush and Miller[3] have shown that the two station extrapolation scheme for foF2 prediction breaks down (correlation coefficient < 0.7) beyond 1800 km in the E-W direction and beyond 1000 km in the N-S direction. The distance for which the correlation coefficient equals 0.7 is subse-

---

1. Barghausen, A.L., Finney, J.W., Proctor, L.L., and Schultz, L.D. (1969) Predicting Long Term Operational Parameters of High Frequency Sky-Wave Telecommunications Systems, ESSA Technical Report ERL 110-ITS78.
2. Lloyd, J.L., Haydon, G.W., Lucas, D.L., and Teters, L.R. (1978) Estimating the Performance of Telecommunication Systems Using the Ionospheric Transmission Channel, National Telecommunications and Information Administration, Boulder, Colo.
3. Rush, C.M., and Miller, D. (1973) A Three-Dimensional Ionospheric Model Using Observed Ionospheric Parameters, AFCRL-TR-73-0567, AD 772672.

quently referred to as the correlation distance. Davis and Rush[4] studied correlations using European and American stations as well as the net of Russian ionospheric stations for prediction of foF2 during the sunrise transition period. They conclude that the extrapolation scheme of predicting foF2 for the OTH-B coverage area on the East Coast of the United States from observations at European stations does not work. There is an additional complication because the reflection points of interest to the OTH-B coverage and the corresponding European stations are at the same geographic (solar influence) latitude but are at quite different geomagnetic (auroral/trough influence) latitudes.

The ionospheric reflection region of an OTH-B radar is typically 1000-1250 km away from the transmitter. For spatial extrapolation from the radar ionosonde to the ionospheric reflection region, this separation distance barely satisfies the correlation range determined by Rush and Miller[3] depending on the direction (N-S, E-W) of radar illumination. In addition, the sunrise observations at the East Coast Radar Site will be at the same time (along the N-S meridian), or at a later time, but never earlier than sunrise in the OTH-B reflection regions. Thus, even for real time specification, the vertical ionosonde observations from the transmitter site have to be extrapolated both in time as well as in distance in applying the two station method for OTH-B coverage. Prediction must still be made for the next hour(s). The result of such a scheme may be acceptable for non-transition periods but is not useful for the transition period in the view of the Rush and Miller[3] and Davis and Rush[4] investigations.

To obtain foF2 measurements for better real-time specification of the ionosphere, and other requirements such as the reliable h'(f) determination at key locations, ionosondes have been deployed at Goose Bay (GS), Labrador, and Argentia (AG), Newfoundland, and deployment is planned for ionosondes at Bermuda (BR) and Wallops Island, Va (WA). These stations will provide real-time ionospheric data from under or close to the OTH midpoint areas for the East Coast system. (See locations with respect to the midpoint ionosphere shown in Figure 1.) This will eliminate or greatly reduce the need for spatial extrapolation of the observations, making these data very reliable for updating of the OTH-B virtual height/-coordinate conversion tables. However, for the period of fast foF2 changes, a better short term prediction scheme is still needed to guide the frequency manager in the necessary rapid frequency selection. Therefore, this study was conducted to find a suitable approach of predicting foF2 from prior days' and real time foF2

---

4. Davis, R.M., Jr., and Rush, C.M. (1983) Feasibility of Forecasting foF2 Disturbances During the Sunrise Transition Period, Technical Memorandum Series NTIA-TM-83-87, U.S. Department of Commerce, National Telecommunications and Information Administration.

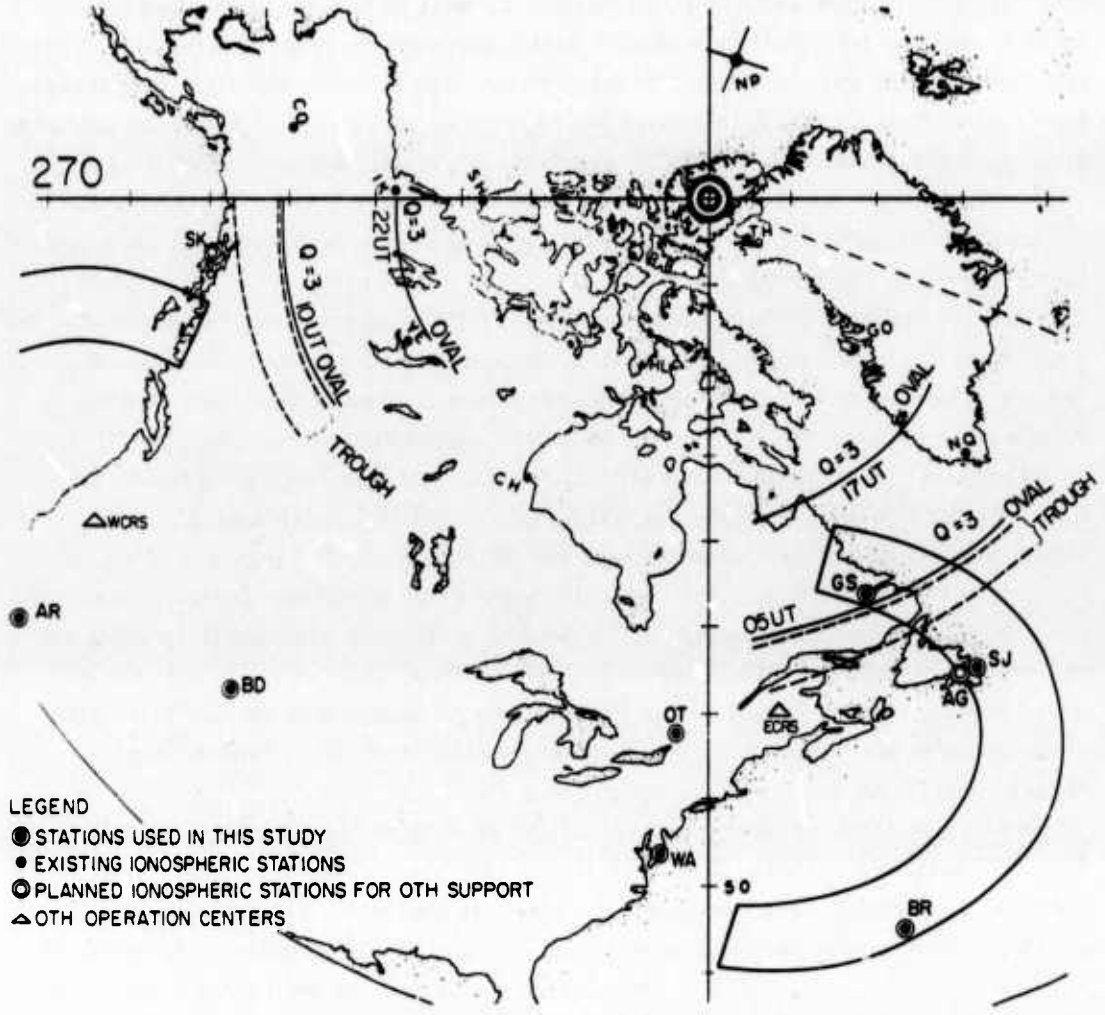

Figure 1. OTH Coverage Area of the East and West Coast Based Radar Systems

observations at these stations within the OTH midpoint area. This report presents the results of the study.

Section 2 defines in detail the problem encountered in radar frequency management during the sunrise period. Section 3 presents the data base used in this study. The different studies, such as the accuracy of IONCAP predictions, the two station method of Davis and Rush,[4] and the study of the scheme proposed in this paper did not always use the same data base. In Table 1, we identify the stations used for the present study as well as those used, in addition or instead, in the other studies.

The analysis in Section 4 presents several new approaches to short term foF2

Table 1. Ionospheric Stations Used in the Analysis

Station	Geographic Latitude	Geographic Longitude	Corr. Geomagnetic Latitude (N)	Corr. Geomagnetic Longitude (E)	ST LT = UT + ΔH ΔH (hr)	Remarks
Narsarssuaq Greenland	61.2N	45.4W	68.9	44.0	-3.0	1, 3
Goose Bay, Canada	53.3N	60.4W	64.9	21.2	-4.0	2
Lindau, Germany	51.6N	10.1E	49.0	87.9	+0.7	3
Slough, England	51.5N	0.6W	50.0	80.4	0.0	3
Dourbes, Belgium	50.1N	4.6E	47.9	83.0	+0.3	3
St. Johns, Canada	47.6N	52.7W	57.6	29.1	-3.5	1, 2
Ottawa, Canada	45.4N	75.9W	58.5	355.7	-5.1	1, 2, 3
Boulder, USA	40.0N	105.3W	49.3	315.7	-7.0	1
Wallops, USA	37.8N	75.5W	51.1	355.4	-5.0	1, 2
Arguello, USA	35.6N	120.6W	41.3	300.9	-8.0	2

1. Stations used for proposed prediction scheme.
2. Stations used for long term accuracy of IONCAP predictions.
3. Stations used by Davis and Rush[4] for two station method.

predictions that were evaluated for usefulness, such as the use of prior days' average foF2 at the corresponding LT, or the combination of previous day(s) hourly slope of foF2 with the last observed foF2 for a 1-hr prediction. As a baseline, to judge improvement of the short term predictions, we determined prediction errors using the IONCAP model[2] alone.

This analysis shows that the best prediction for a 1-hr interval is the combination of the currently observed foF2, the average hourly slope determined using foF2 measurements for the past four days, and a correction in the slope as a function of the deviation of the observed foF2 from the past 4-day average foF2 value for the particular hour. The procedure for such prediction of foF2 is summarized in the conclusion.

The Experimental Radar System (ERS) consistently experienced frequency management difficulties during 2-3 hr of the sunrise period, with the system performing poorly for 8 to 12 percent of the operation time on a routine basis. It is essential to realize that these observed difficulties occurring 8 to 12 percent of the time were not a random problem. The improvements possible with the proposed prediction technique should increase the overall performance of the system and at least randomize poor performance in the difficult sunrise period.

2. DEFINITION OF THE SUNRISE foF2 PROBLEM

The foF2 contours for several stations of OTH-B interest are shown in the following figures covering high and low phases of sunspot activity. The stations selected are Goose Bay, St. Johns, Ottawa, Wallops, and Arguello. In the OTH-B coverage area shown in Figure 1, Goose Bay is centered in the northern 30° beam sector of the East Coast Radar System (ECRS). It is located at the equatorward boundary of the auroral oval. The station moves in and out of the auroral region due to rotation of Earth. St. Johns is south of the auroral zone and, at night, lies close to or within the mid-latitude F-layer trough region. Ottawa is at the same C.G. latitude as St. Johns, lies west of the radar coverage, is used to confirm the ionospheric behavior at St. Johns, and replaces St. Johns whenever St. Johns data are lacking. Ottawa is also located at a C.G. latitude similar to Sitka, Alaska, a sounder site selected for the West Coast Radar Systems (WCRS). Wallops represents the center of the southern coverage area of 180° from the ECRS and is unaffected by auroral or ionospheric trough phenomena. Arguello represents the ionospheric conditions for large parts of the coverage region of the WCRS and for the southernmost beams of the ECRS. Thus, these stations cover most of the midpoint ionospheres relevant to the east and west coast radars.

The foF2 contours from the monthly median observations and from the IONCAP monthly predictions are shown for Goose Bay, St. Johns, Ottawa, Wallops, and Arguello in Figures 2a-2e, for the high sunspot activity (SSN = 160) period from June 1979 to June 1980. Figures 3a-3d cover the low sunspot activity (SSN = 14) period for the calendar year 1976. No data are available from Arguello in 1976. In each figure, the bold lines show the IONCAP[2] monthly median predictions (using the observed smoothed sunspot number), and the dashed lines show the monthly median observations. The monthly median observations are derived from the routine hourly ionospheric soundings from the stations.

The features common to all these figures are: (1) a good agreement (within ±1 MHz) between predictions and observations; (2) the bunching of the contours in winter months both predicted and observed in the 06-08 LT time window showing a rapid increase in foF2 during the sunrise hours; (3) a factor of 2 increase in noon foF2 from sunspot minimum to sunspot maximum; and (4) the presence of a strong sunrise transition in foF2 for all the winter months independent of the phase of the solar cycle activity. The figures show that although the models reproduce most of the observed foF2 behavior, they are unable, even in the median, to provide the prediction accuracy of $\leqslant$ 0.5 MHz needed in real time by the operational systems during sunrise periods. The general accuracy of IONCAP monthly median foF2s is ±1 MHz, and somewhat worse for sunrise transition periods, when compared to the median of the observed data.

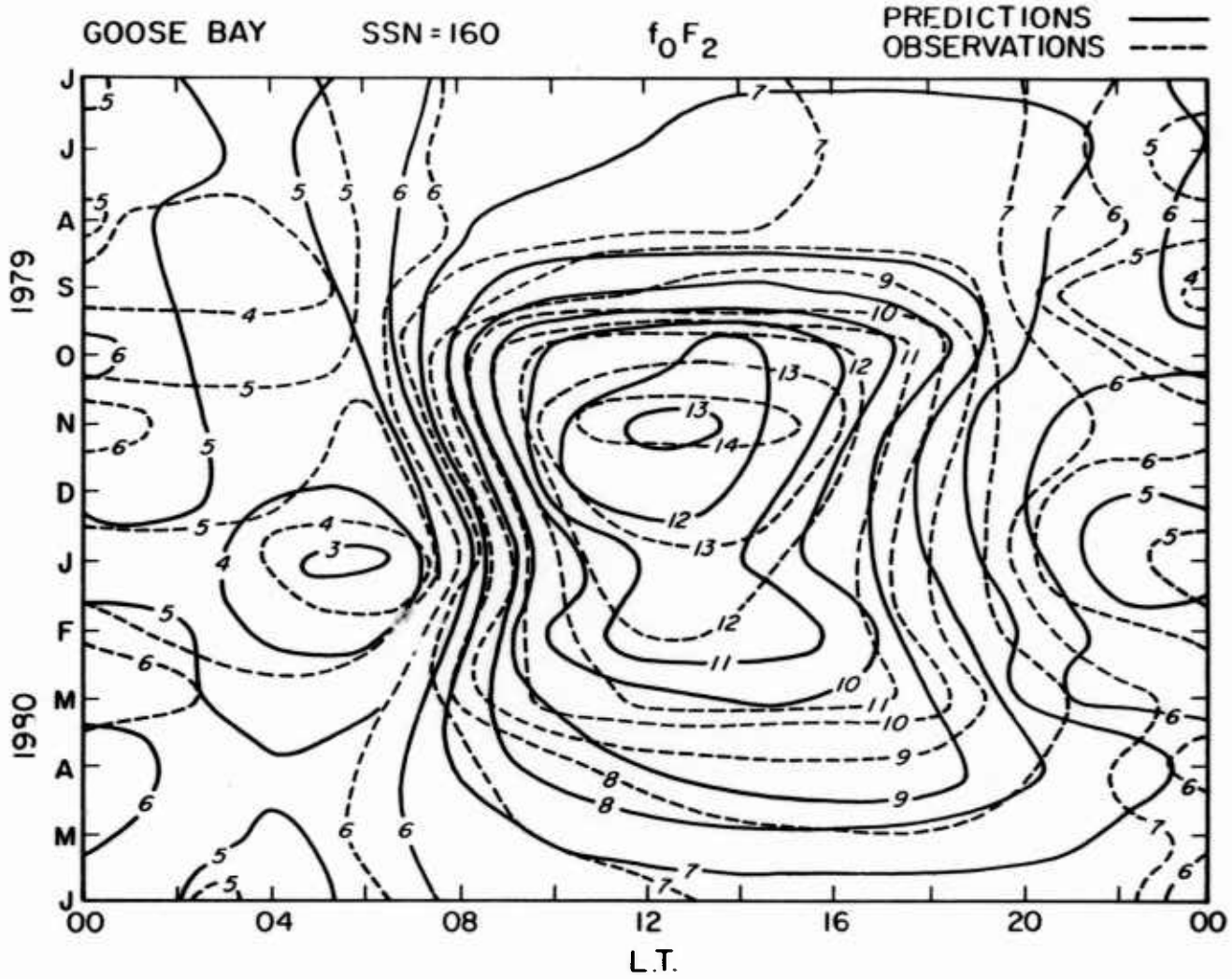

Figure 2a. Monthly Median Contours of foF2 for High Sunspot Activity (SSN = 160) for Goose Bay

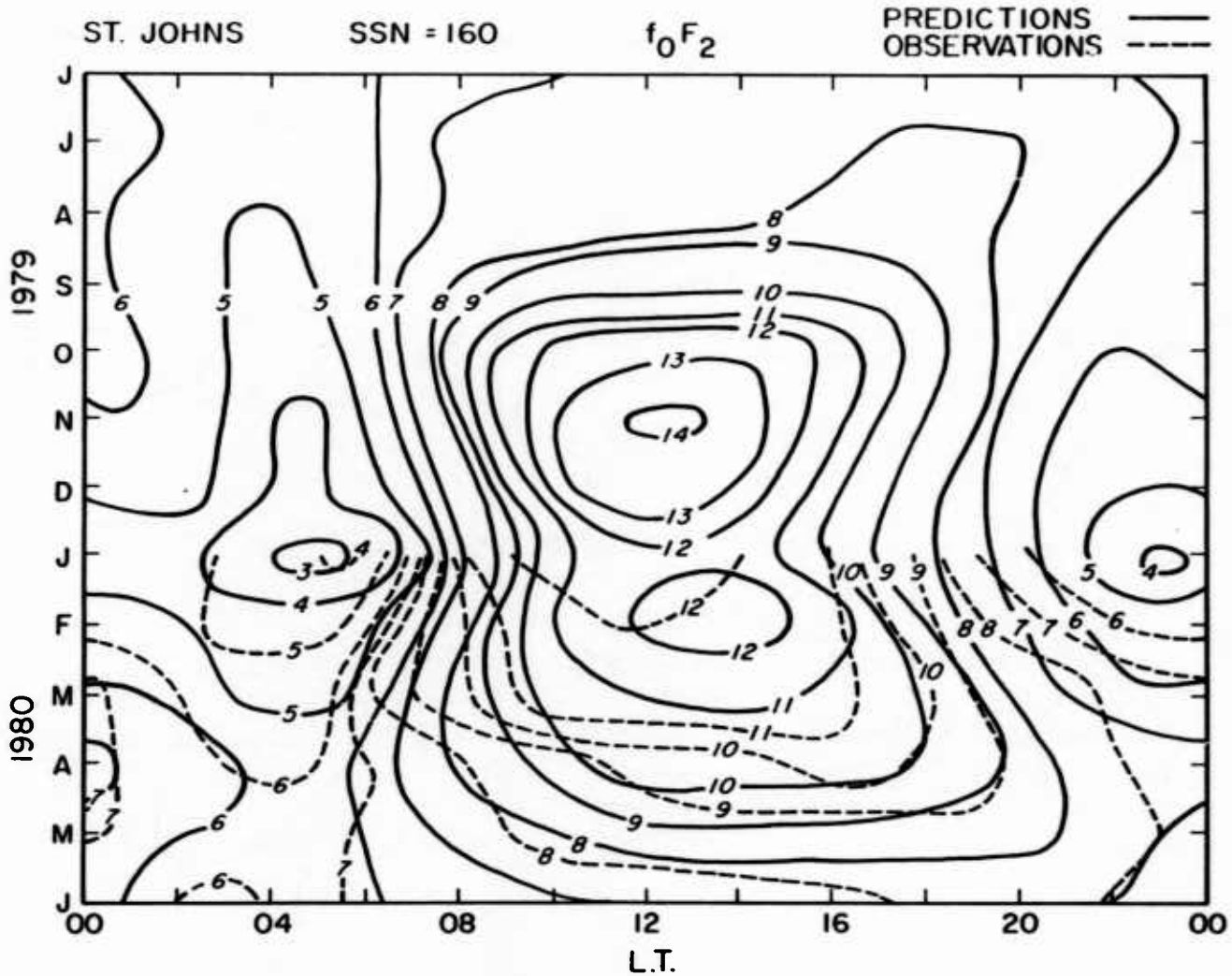

Figure 2b. Monthly Median Contours of foF2 for High Sunspot Activity (SSN = 160) for St. Johns

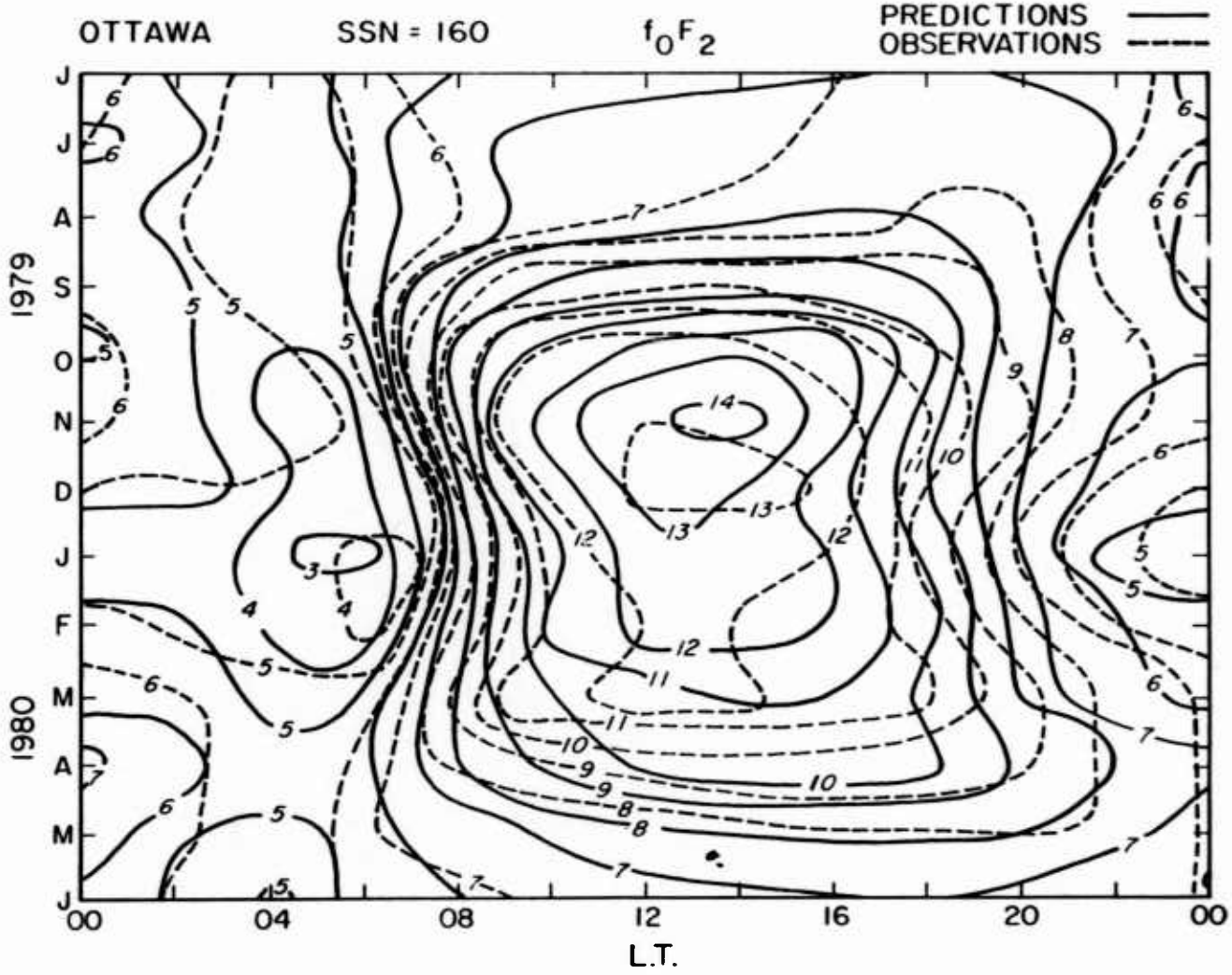

Figure 2c. Monthly Median Contours of foF2 for High Sunspot Activity (SSN = 160) for Ottawa

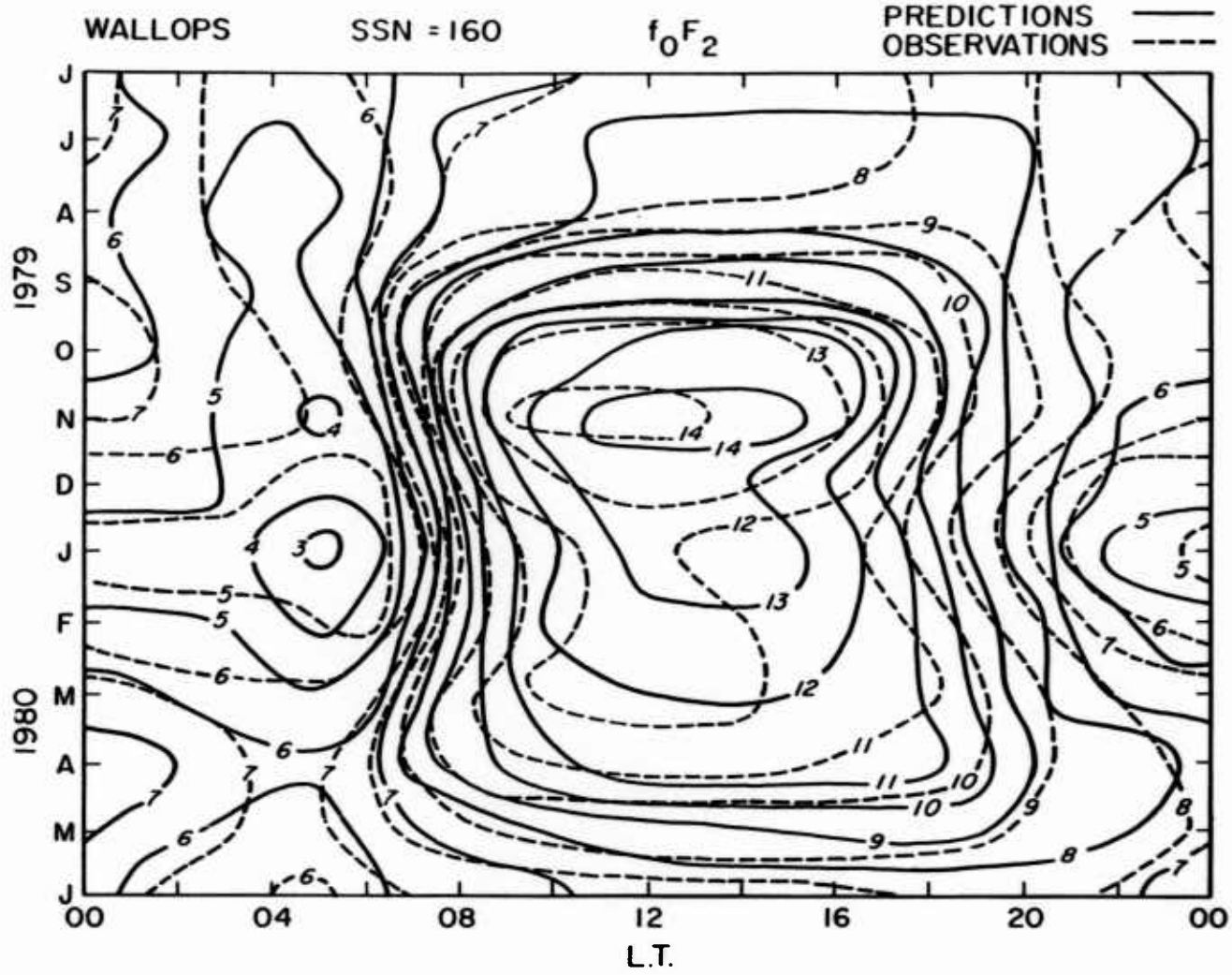

Figure 2d. Monthly Median Contours of foF2 for High Sunspot Activity (SSN = 160) for Wallops

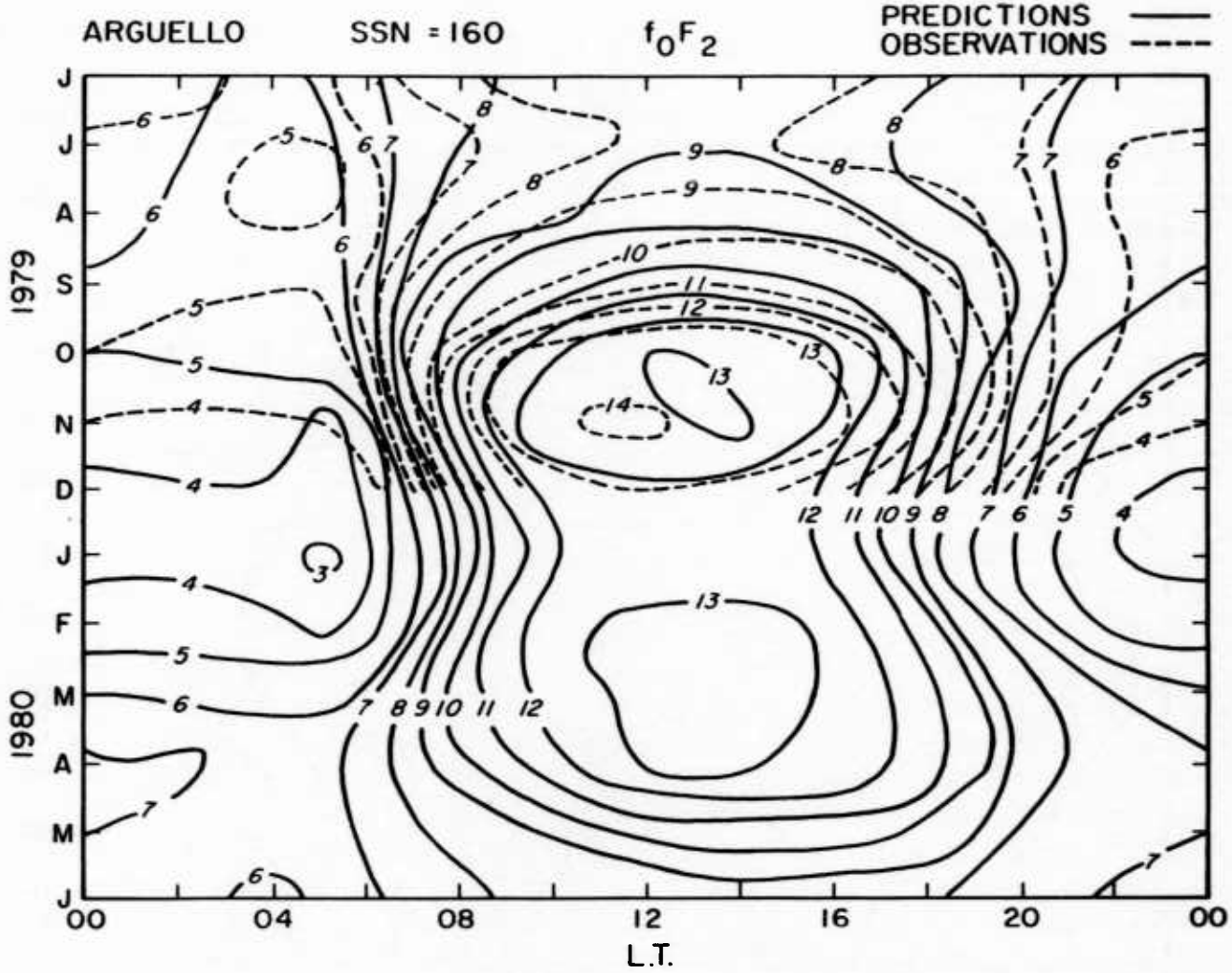

Figure 2e. Monthly Median Contours of foF2 for High Sunspot Activity (SSN = 160) for Arguello

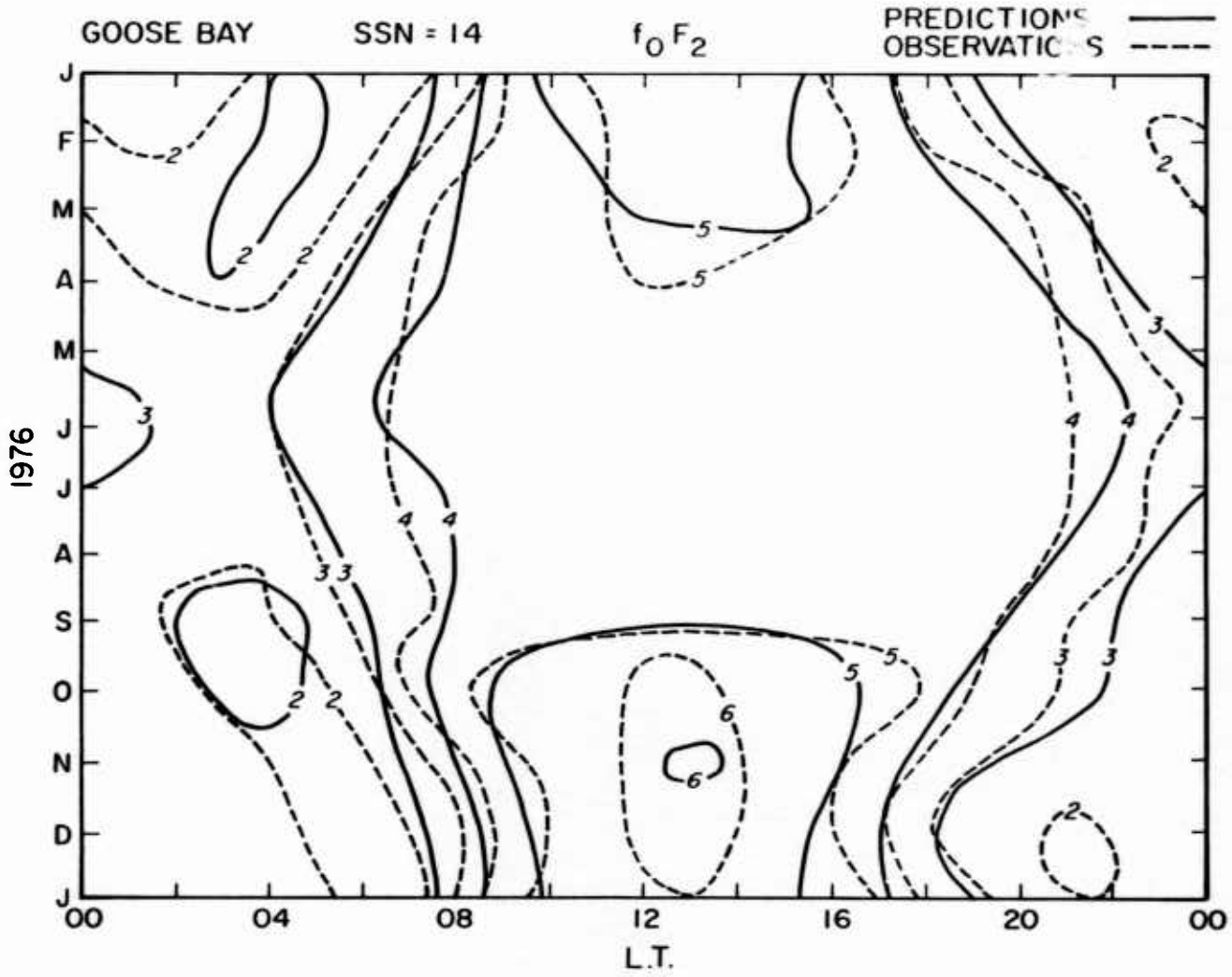

Figure 3a. Monthly Median Contours of foF2 for Low Sunspot Activity (SSN = 14) for Goose Bay

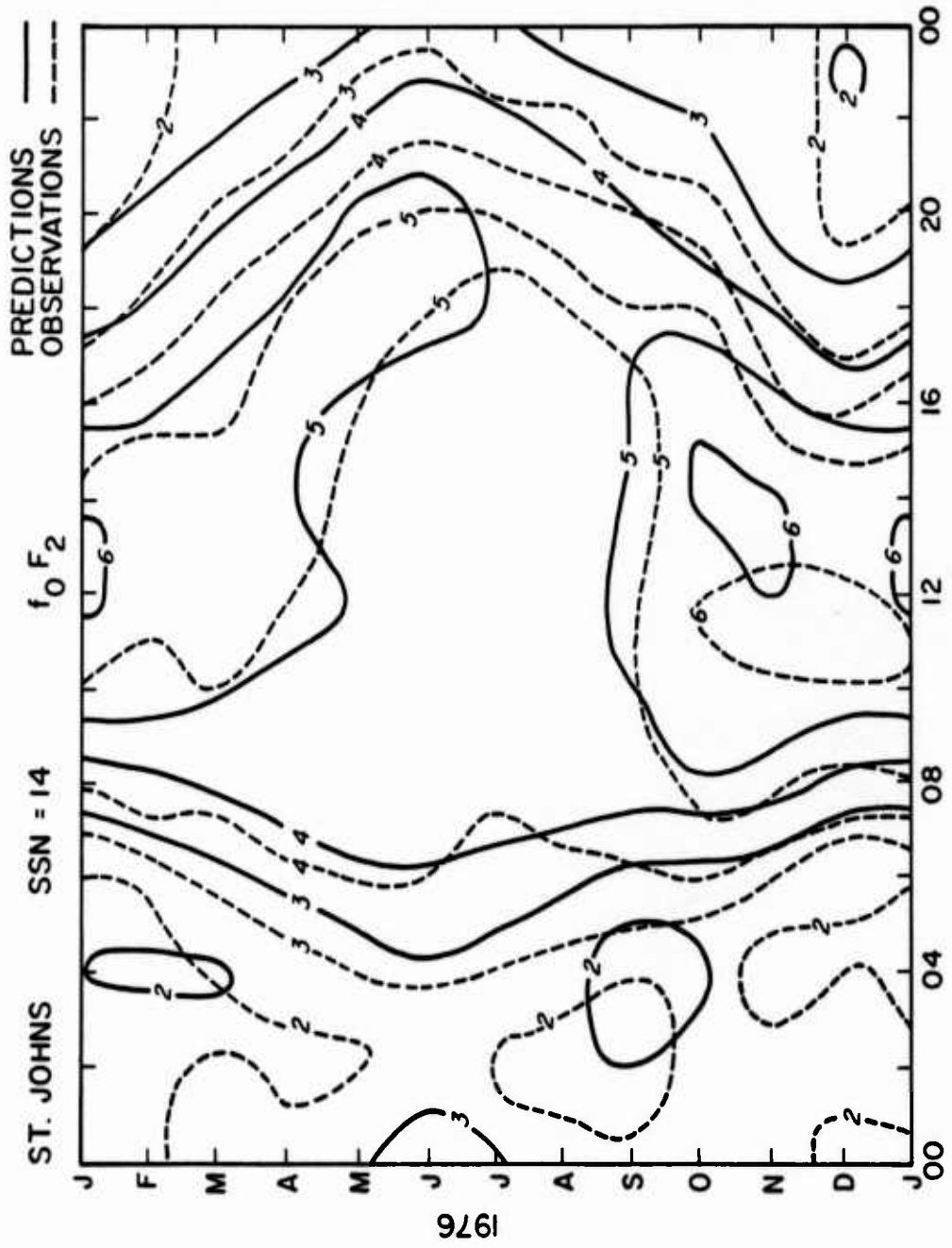

Figure 3b. Monthly Median Contours of foF2 for Low Sunspot Activity (SSN = 14) for St. Johns

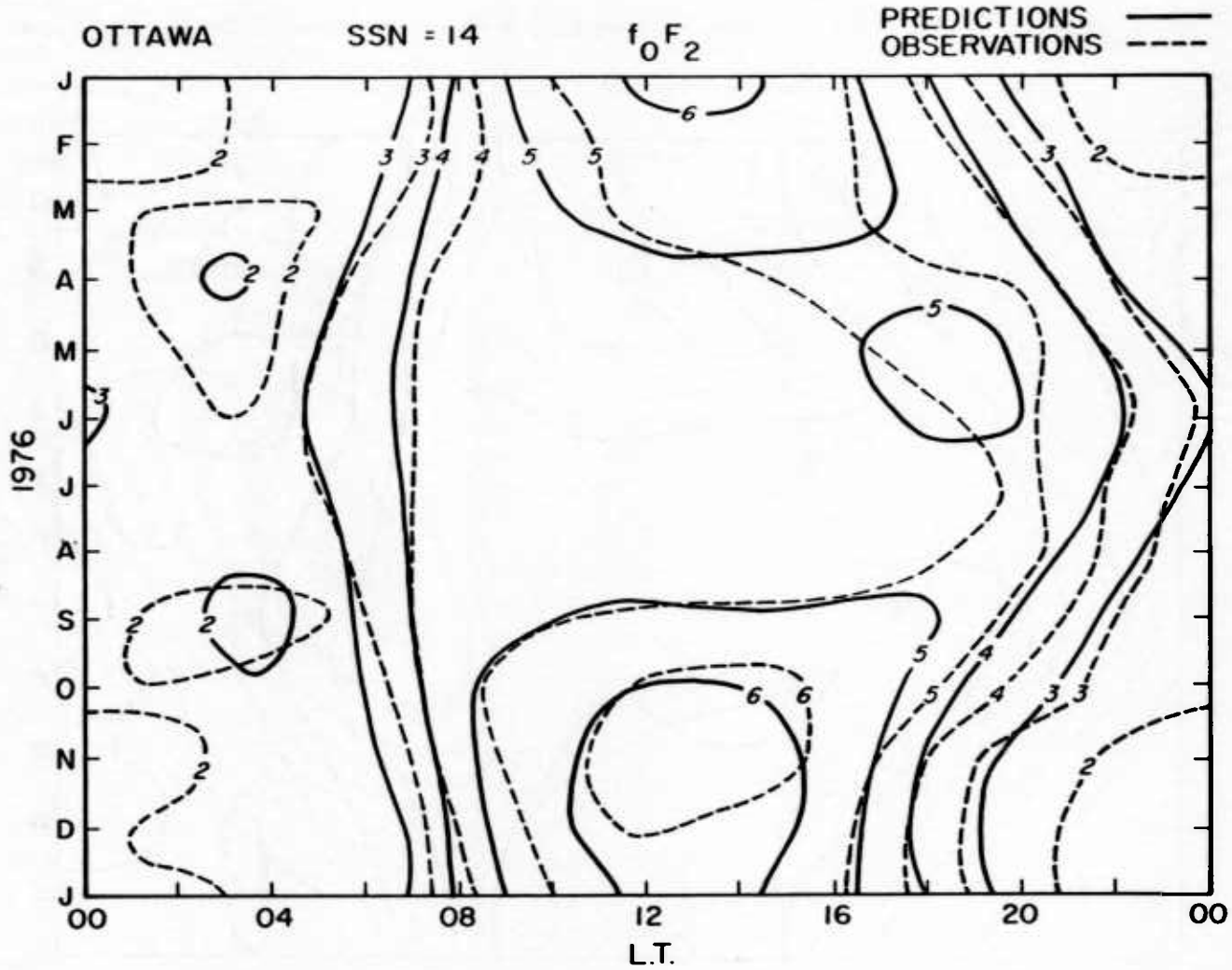

Figure 3c. Monthly Median Contours of foF2 for Low Sunspot Activity (SSN = 14) for Ottawa

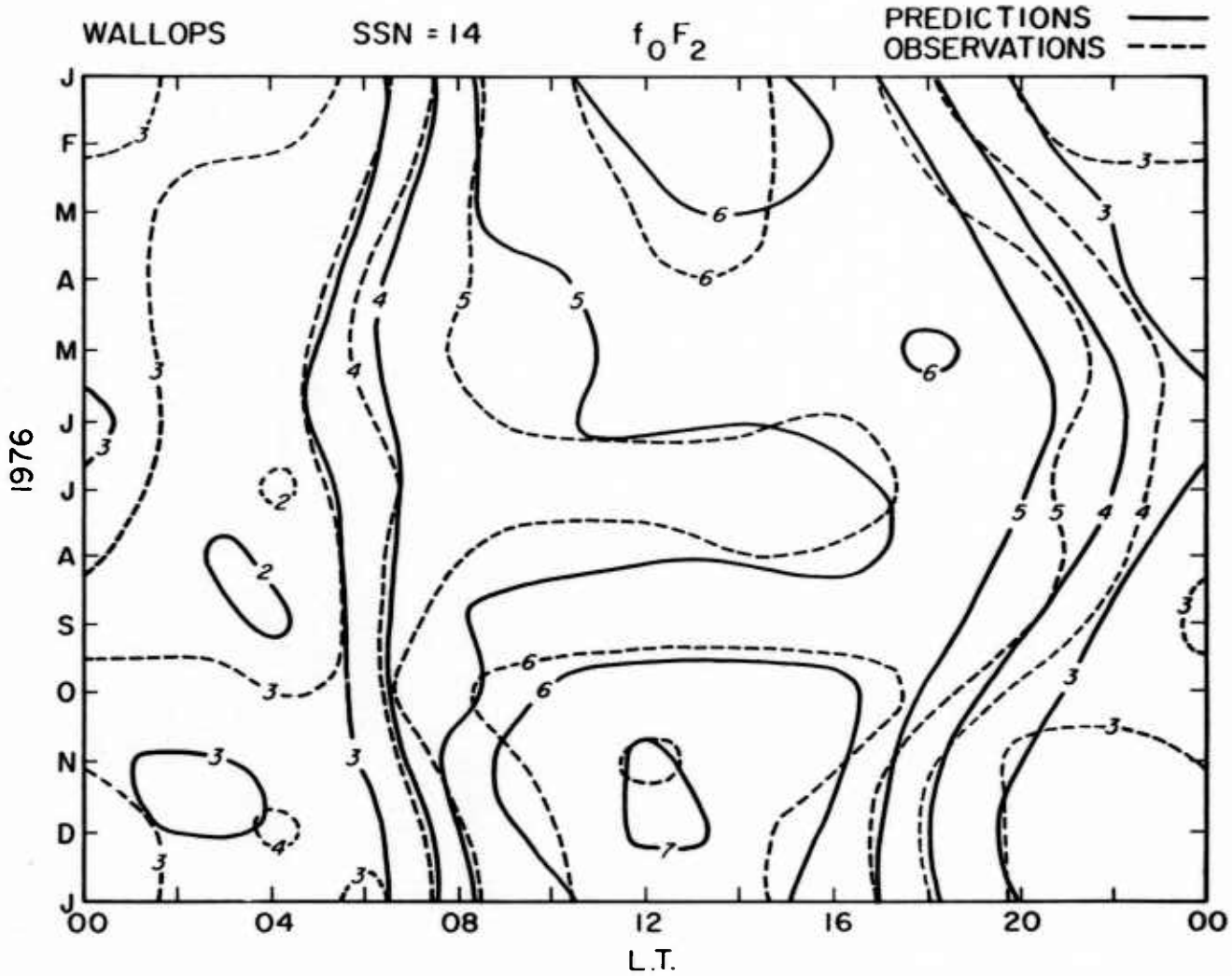

Figure 3d. Monthly Median Contours of foF2 for Low Sunspot Activity (SSN = 14) for Wallops

For determining the rapid change in foF2 (from Figures 2 and 3) during sunrise, a quantitative measure P_i is defined as the percentage in change of foF2 over 1 hr,

$$P_i = 200 \times \frac{(foF2_{i+1} - foF2_i)}{(foF2_{i+1} + foF2_i)} \quad (1)$$

where $foF2_i$ refers to the hourly observations at a station at the ith hour. This percent change in foF2 is shown for the sunrise period in Figure 4 for high sunspot activity (SSN = 158) and in Figure 5 for low sunspot activity (SSN = 17).

These figures show that during sunrise, gradients $\geqslant$ 20 percent last for about 3 hr. This rapid increase in foF2 is present for at least 8 months (centered on winter) of the year. Gradients as high as 60 percent per hour for short periods are present in some months. In years of low sunspot activity, Goose Bay (Figure 5) also shows a 30 percent gradient in foF2 during sunset hours in the winter months. None of the other stations show a similar rapid foF2 change during sunset.

The radar operation frequency is related to the midpoint foF2 by the equation,

$$f_{RADAR} = foF2 \times M \quad (2)$$

where the multiplying factor M is a function of h_m and y_m (the height and thickness of the layer) and the range to the barrier. To accommodate the rapid increase in foF2 during sunrise, the operating frequency of the radar has to be changed in step with the sunrise changes in foF2. The factor relevant to the frequency management is the M factor, which changes with skip distance. To simplify the discussion, we will consider a parabolic layer shape, an assumption used in the computations presented here (Appleton and Beynon[5]). While other layer shapes may slightly alter the M factor for a given skip distance, the general conclusions are not affected.

The M factors covering representative ranges of h_m, h_o, and y_m, computed from equations by Appleton and Beynon,[5] are shown in Figure 6. For the ratio y_m/h_o, we have chosen a range from 0.4 to 0.6 covering a large range of ionospheric conditions. With y_m/h_o = 0.4, the figure shows four curves for h_m = 250, 300, 350, and 400 km. The layer parameters h_m, h_o, and y_m used in the mathematical formulation are interconnected, y_m and h_o by the selected ratio, and h_m by the relation $h_m = h_o + y_m$. For y_m/h_o = 0.6, the resulting M factor

5. Appleton, E.V., and Beynon, W.J.G. (1940) The application of ionospheric data to radio communication problems, Part I., Proc. Phys. Soc., Part I, 52:518.

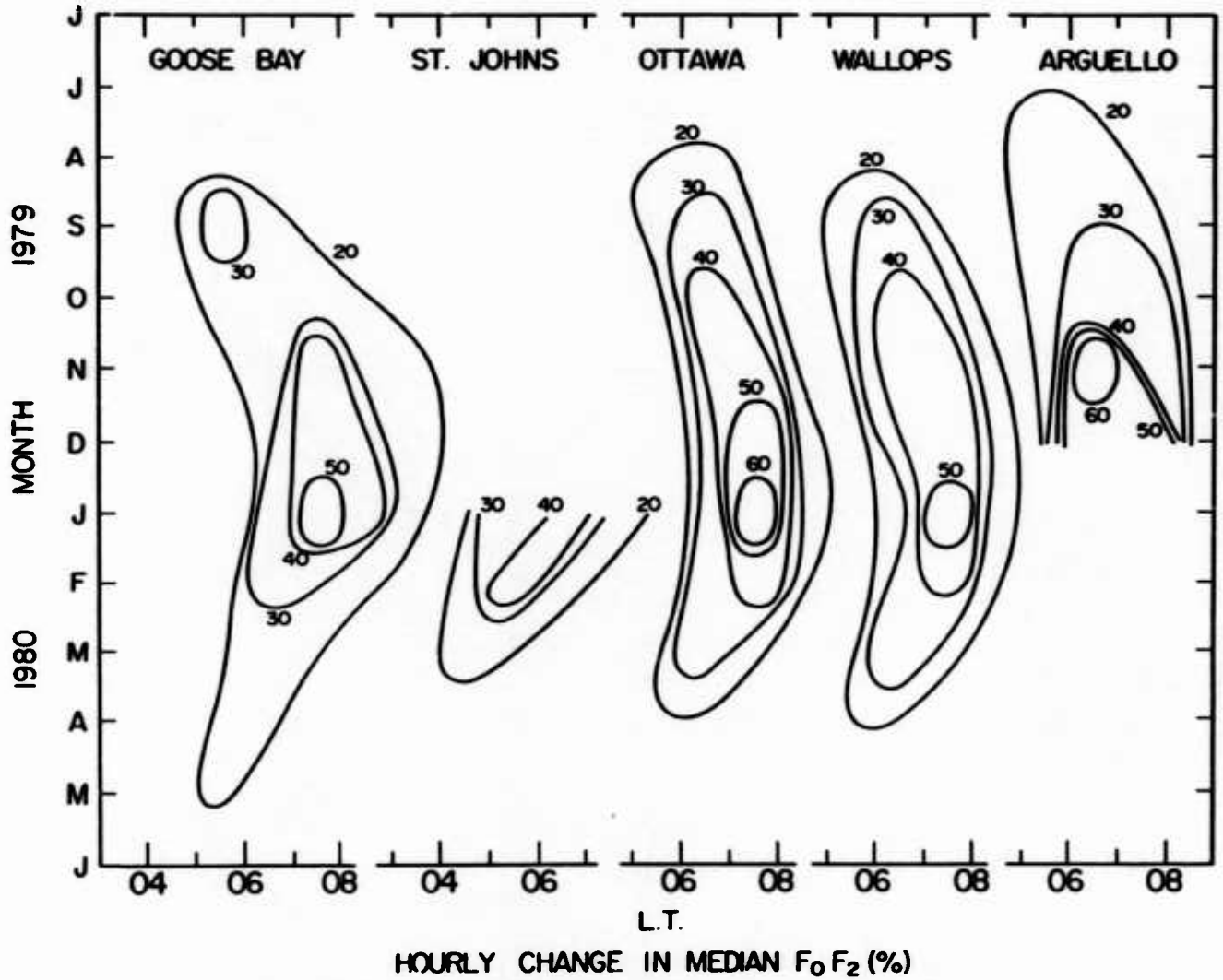

Figure 4. Percent Increase in foF2 During Morning Hours for High Sunspot Activity

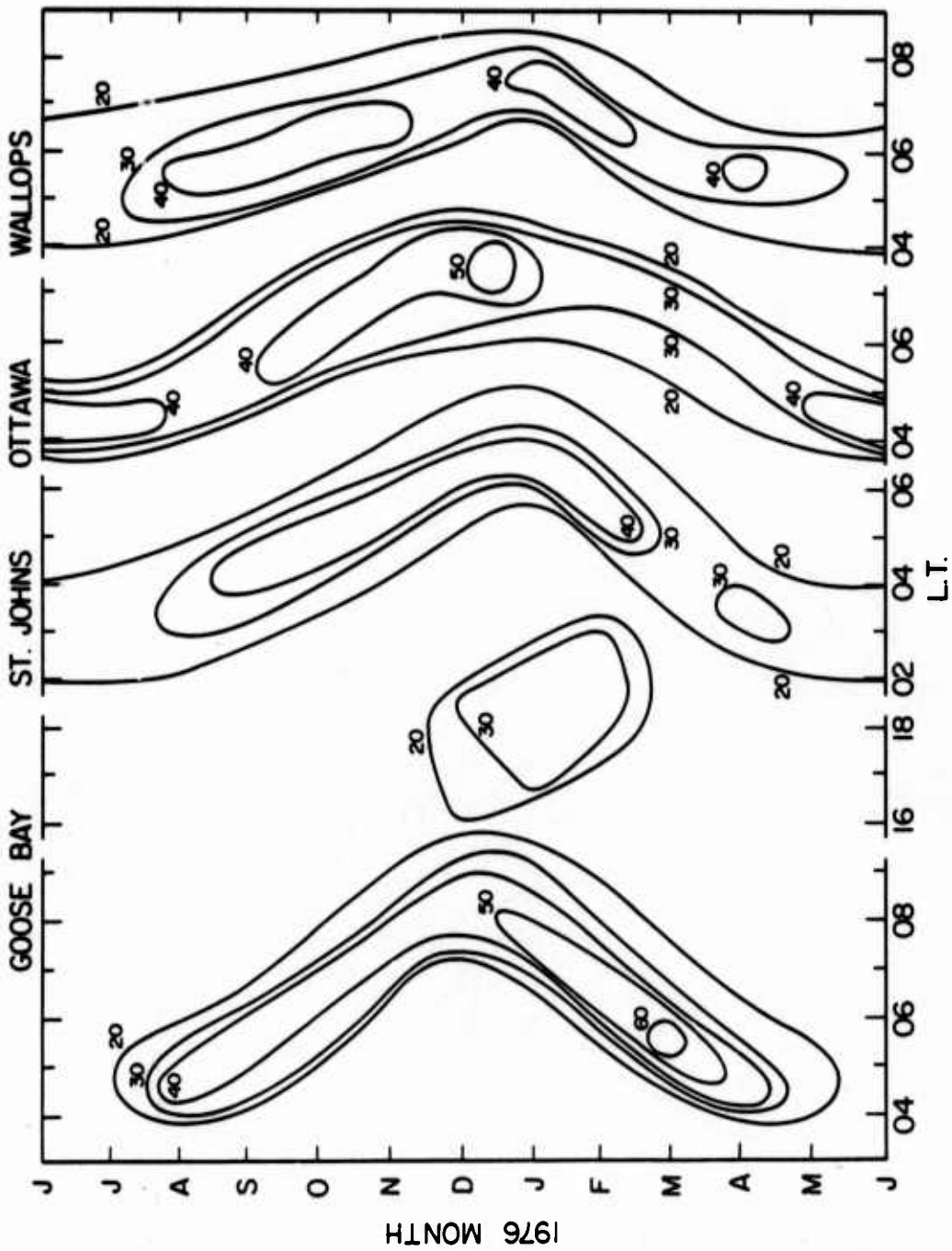

Figure 5. Percent Increase in foF2 During Morning Hours for Low Sunspot Activity

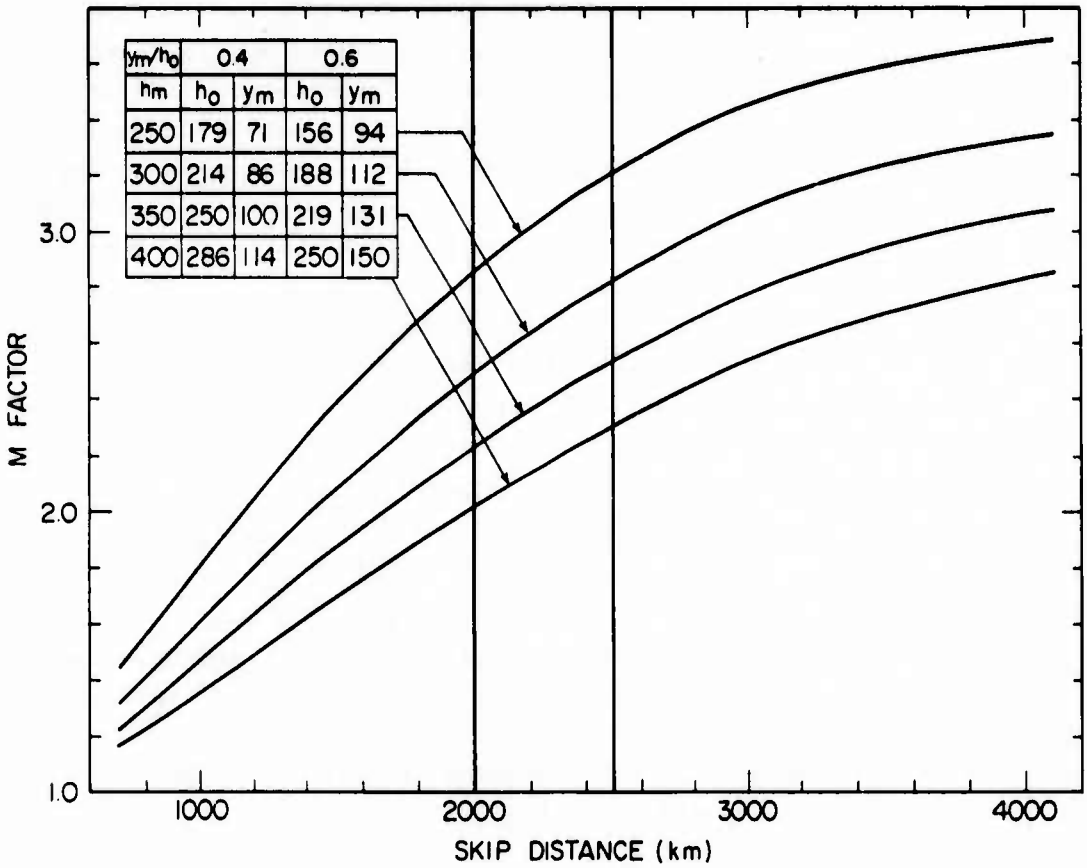

Figure 6. Dependence of M Factor on Skip Distance for y_m/h_o = 0.4 and 0.6 Respectively

values as a function of range are about 2 percent lower than those for y_m/h_o = 0.4. Therefore, only one set of curves was plotted. The y_m and h_o values computed for each selected h_m are tabulated separately for y_m/h_o = 0.4 and 0.6 in the figure. The planned location of the barrier at 2000-2500 km for the sunrise period is shown by vertical lines in the figure.

The ratios 0.4 and 0.6 refer to thinner and thicker F-layers respectively. With the diurnal variation of h_m, higher at night and lower at noon, the lower curves represent night conditions, and the upper curves represent noon conditions. In seasonal variation, h_m is higher in summer than in winter. Similarly, with respect to solar cycle activity, the upper curves refer to low sunspot activity, and the lower curves refer to high sunspot activity (at low sunspot activity, h_m is lower than at high sunspot activity). In descending order of importance, the terms dominating the M factor are skip distance, h_m, and y_m/h_o. The slope of the M factor is larger at small skip distances and becomes smaller as the distance in-

creases. In Figures 2 through 5 and the related discussions, we have considered only the variations of the foF2 median values at sunrise periods and have not taken into account the parameters h_m, h_o, and y_m, which also change during the sunrise period of 2-3 hr. During the sunrise period of 2-3 hr, the F-layer comes down by about 40 km (computed from IONCAP model) at the midpoint of the barrier distance (2000-2500 km). The M factor would correspondingly increase by 10 percent as seen from Figure 6.

For practical purposes, y_m/h_o = 0.4 to 0.6 covers most of the full range of ionospheric changes expected during sunrise with four curves. One would mostly be working within the bounds of a neighboring pair of curves. For example, on a morning in a winter month with high sunspot activity, SSN = 160, IONCAP model computations provide the following layer parameters:

LMT	h_m (km)	y_m (km)	h_o (km)	y_m/h_o
06	355	99	256	0.39
10	299	104	195	0.53

To interpret these changes, one would work in the bounds of the middle pair of curves, with the starting and ending M factors of 2.2 and 2.9 for the midpoint of the barrier.

One way of looking at the effects of the changing ionosphere on the radar situation is to start from the relation

$$\frac{f_{RADAR}}{foF2} = M\ (Distance,\ h_m,\ h_o,\ y_m). \tag{3}$$

Keeping all layer parameters (except foF2) and the radar frequency fixed and increasing (decreasing) foF2 at the midpoint at sunrise (sunset) causes the M factor to decrease (increase). As Figure 6 shows, this causes the skip distance and therefore the barrier to move in (out). This fact combined with the speed with which foF2 changes during sunrise is the main reason for the need to develop a short term prediction scheme.

To look at the effect of h_m, let us keep foF2 and the radar frequency, and therefore the M factor, constant. Lowering (raising) the layer height during sunrise (sunset) decreases (increase the skip distance and therefore the distance to the barrier. Therefore, the changes in the F-layer during sunrise (foF2, h_m) both act in the same direction, speeding up the movement of the barrier towards the radar and increasing the need to change frequency to maintain the barrier at the desired range, while providing overlap of part of the radar footprint prior to and after a frequency change.

From Figure 6, the change in M factor per 100 km range change is computed

as a function of skip distance and is shown in Figure 7. The figure shows that the percentage change in M factor as a function of skip distance is the same for any layer height for skip distances greater than 2000 km. Naturally, this does not imply that the M factor itself is not changing as the layer altitude increases. Figure 6 clearly shows the change of M with the change in h_m.

The change of M with skip distance decreases as the skip distance increases. At the center of the barrier, the change of M is 2.35 percent per 100 km movement of the barrier. Thus, the 250 km (or 1/2 barrier width) allowable sliding of the barrier corresponds to a 6 percent change in M factor. Therefore, to maintain a 50 percent overlap of the barriers through a frequency change, the radar

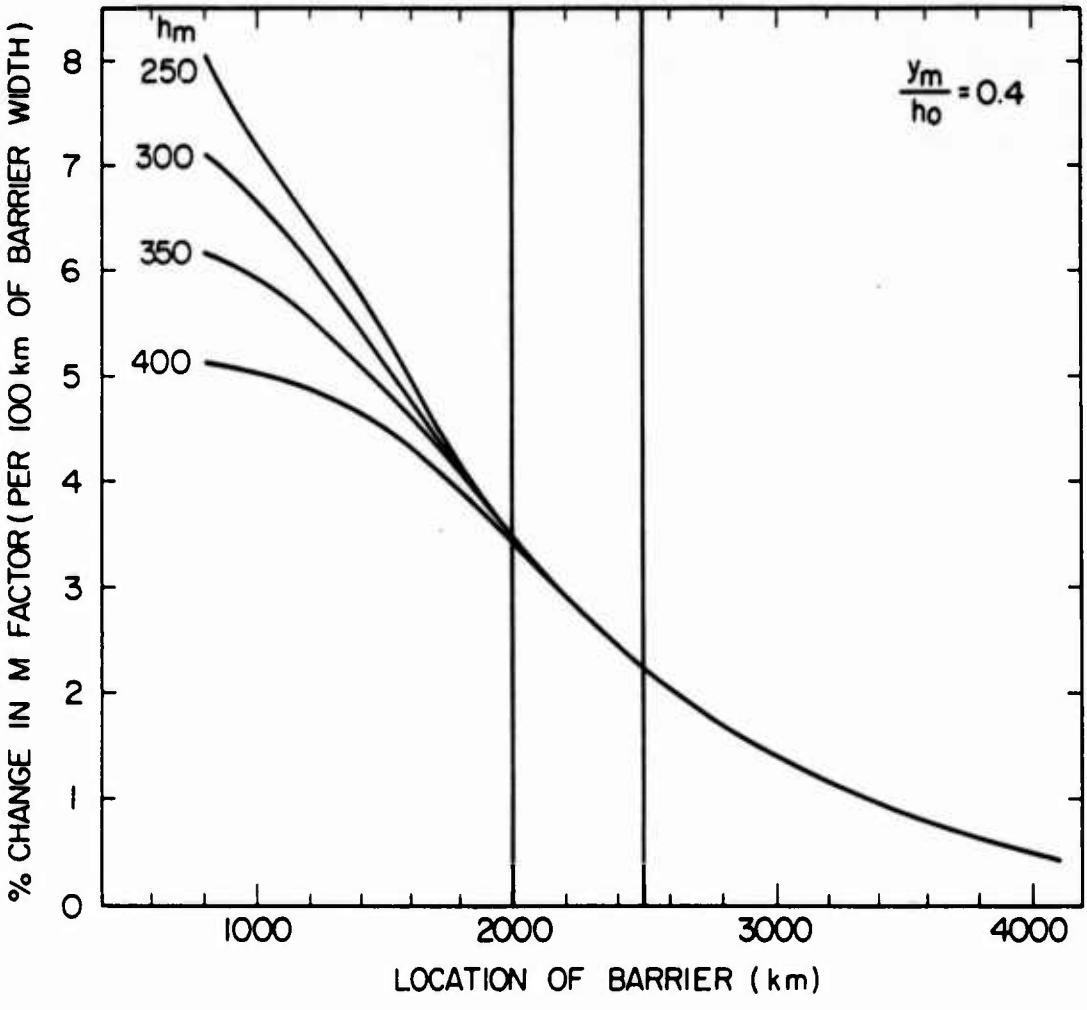

Figure 7. Percent Change in M Factor With Skip Distance

operating frequency has to be changed whenever the change in M factor is larger than 6 percent. Figures 5a and 5b show that the frequency has to be changed 5-10 times per hour to cover the 30-60 percent hourly change in foF2 during sunrise hours. This is equivalent to a change in radar frequency every 6-12 min. Additional changes are required due to the simultaneous lowering of the layer. Such frequent changes demand reliable predictions of foF2.

The data base used in the analysis is presented in the following section.

3. DATA BASE

While defining the sunrise foF2 problem, we have used foF2 median values from several stations (Figures 2 and 3). For investigating hourly foF2 prediction schemes, hourly foF2 data are used from five stations: Narsarssuaq (NQ), St. Johns (SJ), Ottawa (OT), Wallops (WA), and Boulder (BD). These data are representative of the ionosphere in the complete sector of the East Coast OTH-B coverage area (see Figure 1). The geographic and corrected geomagnetic coordinates of all these stations (including those in Figures 2 and 3) are listed in Table 1. Since foF2 observations are routinely presented in UT, but the phenomena depend on local time, the time differences are shown in Table 1. For reference, the European stations used by Davis and Rush[4] for testing the longitudinal extrapolation method are also listed in the table. The selection of stations for this study is guided by the availability of hourly data and by relevance to the ECRS coverage area.

The table shows that the European stations are geomagnetically further south (equatorward) than the OTH-B coverage high latitude stations. Since the ionosphere is controlled by geographic latitude dependent phenomena (solar production, neutral wind systems), as well as by geomagnetic latitude related phenomena (F-trough, auroral oval), it is not surprising that attempts at foF2 predictions for the East Coast Radar, based on foF2 measurements in Europe, were not successful (Davis and Rush[4]). A look at Table 1 shows that the two station method (Davis and Rush[4]) must extrapolate foF2 predictions not only beyond distances greater than 1000 km but also over time differences of 4 hr for the ECRS application.

For the OTH-relevant stations, hourly foF2 data are used for four months: March, June, September, and December, representing the four seasons. To cover the high and low phases of solar cycle activity, the data for calendar years 1969 (average smoothed monthly sunspot number was 100) and 1975 (average smoothed monthly sunspot number was 15) are used. Thus, for each station, the data base consists of 8 mo of hourly foF2 observations. For prediction, it is essential to have a good data base. The sparseness of the present data base is shown by tabu-

lating those periods when observations fall below 10 in any given month (Table 2). The table shows that data suffer severely at Narsarssuaq and partially at St. Johns and at Ottawa. Most of these data are lost because parameters cannot be extracted from ionograms under spread F conditions. It is expected that digital ionosondes[6,7] to be deployed for real time OTH support in the near future will provide a considerably improved capability in terms of spread F performance and better support to proposed prediction schemes as well as the real time OTH-B operation. We do, however, feel that the data base available was sufficient to test the various prediction schemes.

The cumulative distribution of Kp indices from the respective 4 months for 12 hr around sunrise is shown in Figure 8. The magnetic activity is not significantly

Table 2. Months and Stations With Sparse Data Base

Station	Month	Year	Number of Observations L.T. 0	1	2	3	4	5	6	7	8	9	10	11
1) Dourbes	Dec	69											9	9
2) Narsarssuaq	Mar	69	8	8			9							
	Sept	69		7										
	Dec	69	7	5	9									
	Mar	75	4	2	2	3	6	3	8					
	June	75	7	3										
	Sept	75	1	0	1	3	3	7						
	Dec	75	2	2	4	6	7	8	6	4				
3) St Johns	Mar	75		7	8	5	4							
	Dec	75	4	6	7			7	5					
4) Ottawa	Mar	75		9	9	7	5	6						
	Dec	75	8											

6. Reinisch, B.W., Gamache, R.R., Tang, J.S., and Kitrosser, D.F. (1983) Automatic Real Time Ionogram Scaler With True Height Analysis - ARTIST, AFGL-TR-83-0209, AD A135174.

7. Buchau, J., Weber, E.J., Anderson, D.N., Carlson, H.C., Jr., and Moore, J.G. (1985) Ionospheric structures in the polar cap, their relation to satellite scintillations, in the Effect of the Ionosphere on C^{3}I Systems Symposium Proceedings of Ionospheric Effects Symposium, J.M. Goodman, Ed.,

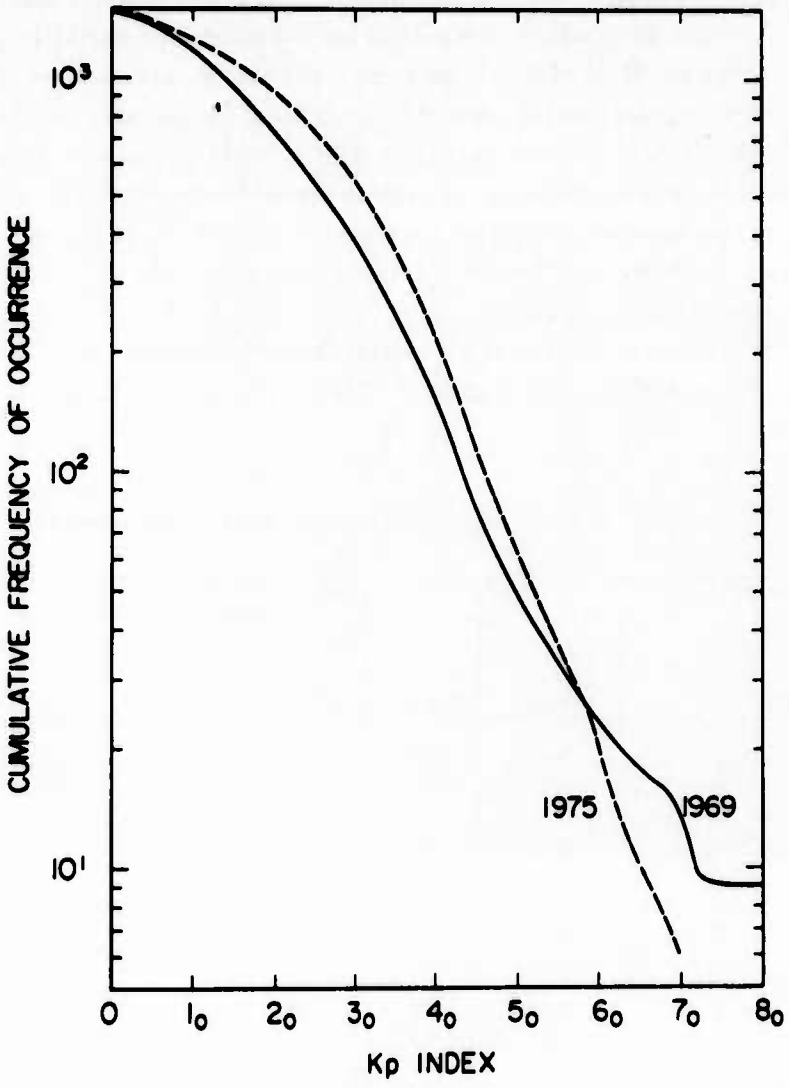

Figure 8. Cumulative Distribution of Kp Index for the Period Selected for Study

different during the periods of high and low solar cycle activity selected in this study. Mendillo et al[8] showed that the effect of magnetic activity on foF2 is not clearly understood and possibly depends on the start time (LT) of the magnetic disturbance. They inspected 28 storms and found, that after a short enhance-

8. Mendillo, M., Lynch, F.X., and Klobuchar, J.A. (1980) Geomagnetic activity control of ionospheric variability, in Prediction of Terrestrial Effects of Solar Activity, Vol. 4 of Solar-Terrestrial Predictions Proceedings, R.F. Donnelly, Ed., Space Environment Laboratory, National Oceanic and Atmospheric Administration, Boulder, Colo.

ment at the start of the storm, foF2 is subsequently depressed over a period of several days. The present study confirms these findings, showing that on highly disturbed days [5 per month identified by World Data Center (WDC), Boulder, Colorado], the respective foF2 values are usually below the observed monthly median foF2s. However, a quantitative relation between Kp and the respective hourly foF2 has not been found.

Since we plan to use predictions from ionospheric models in the analysis, the sunspot number predicted by WDC Boulder (1 month in advance), and the observed sunspot numbers for the 8 mo covered in the analysis, are listed in Table 3. Between high and low solar activity, the sunspot numbers changed by a factor of 10.

Table 3. Sunspot Activity for the Selected Period

Year	Month	Prediction (1 Month Before)	Observed
1969	March	99.8	135.8
	June	106.3	106.0
	September	101.9	91.3
	December	96.4	97.9
1975	March	23.0	11.5
	June	18.3	11.4
	September	15.7	13.9
	December	14.4	7.8

1. ANALYSIS AND DISCUSSION

While considering the constraints in maintaining the barrier range, we have seen that the major concern is in the rate of change in foF2, rather than in the absolute value of foF2. The variation in foF2 for two stations, St. Johns and Wallops, representative for the northern and central ionosphere of the ECRS, is shown in Figures 9 to 12. Similar variations are observed at all the stations.

Each of these figures is divided into two sections along the vertical. The left-hand section presents results from analysis for St. Johns and the right-hand section shows results for Wallops.

The diurnal variation of foF2 during the morning transition for the equinoxes

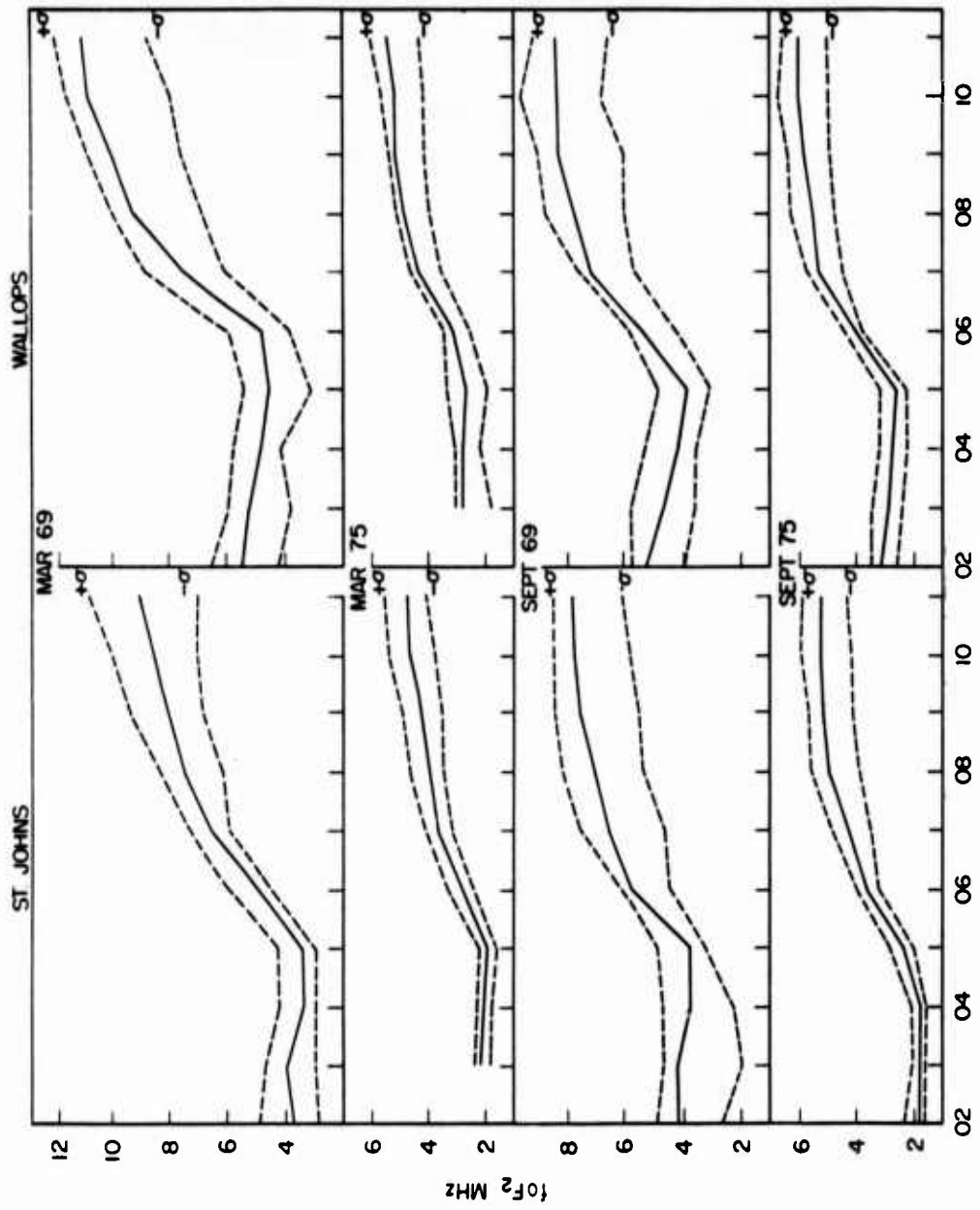

Figure 9a. Diurnal Variation of foF2 in the Morning for Eqinox

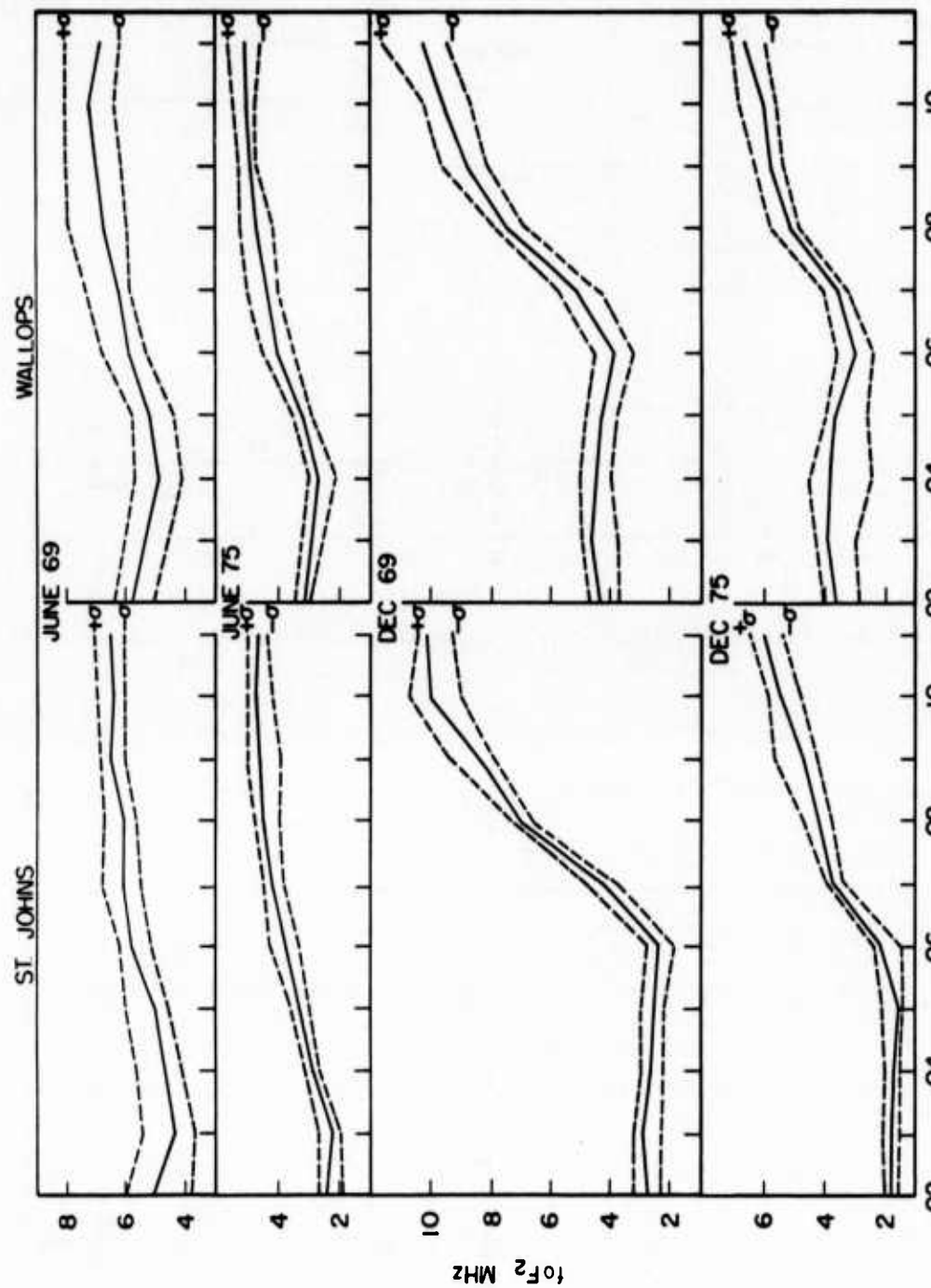

Figure 9b. Diurnal Variation of foF2 in the Morning for Solstice

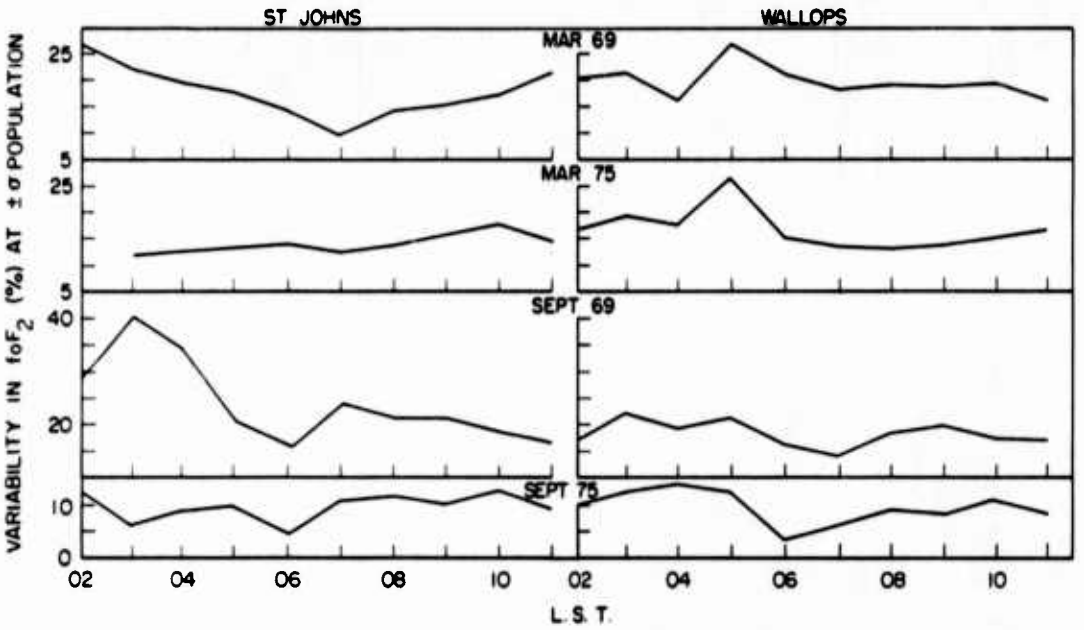

Figure 10a. Percent Variation of foF2 in the Morning Hours for Equinox

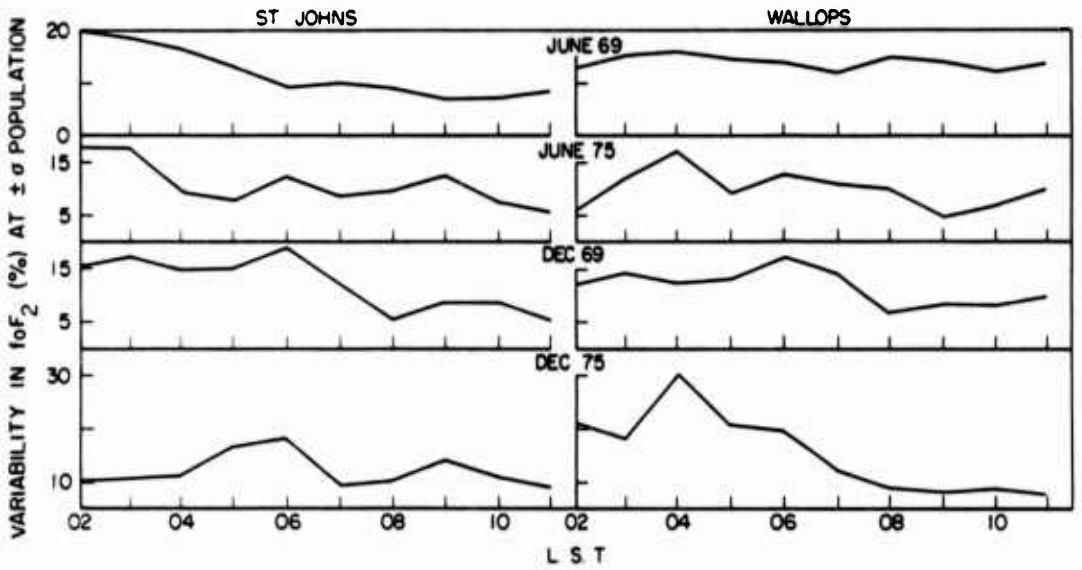

Figure 10b. Percent Variation of foF2 in the Morning Hours for Solstice

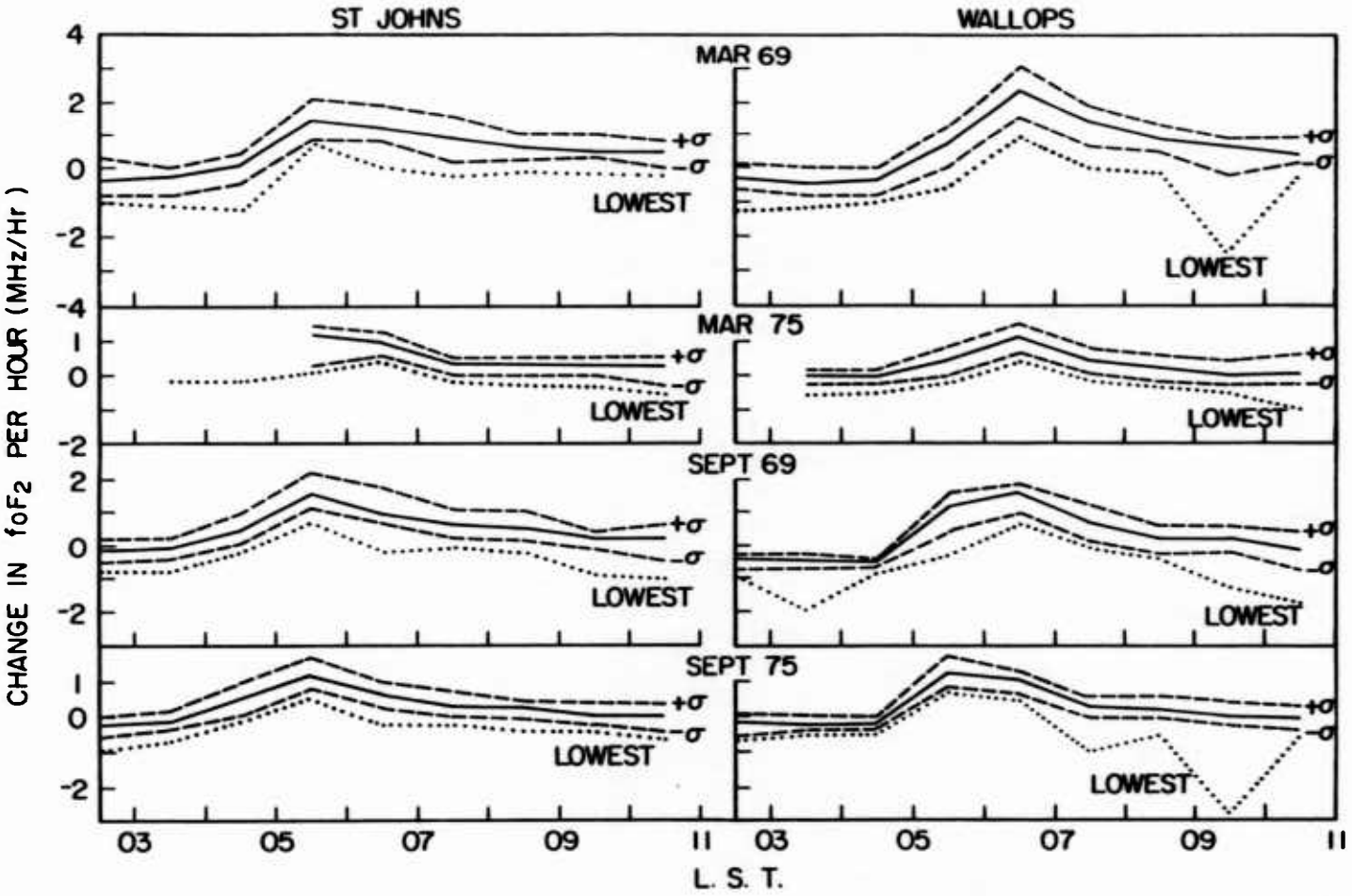

Figure 11a. Hourly Change (Slope) of foF2 in the Morning Hours for Equinox

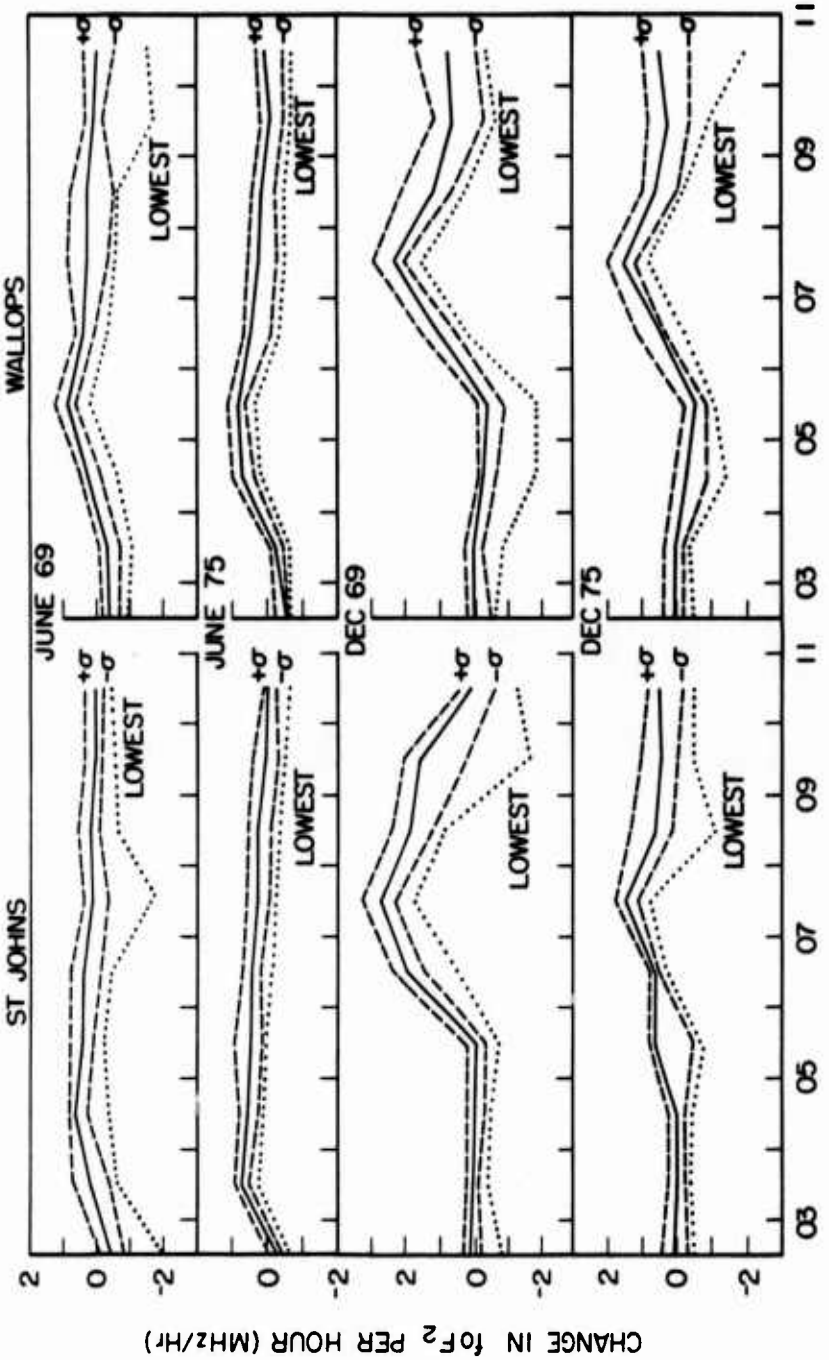

Figure 11b. Hourly Change (Slope) of foF2 in the Morning Hours for Solstice

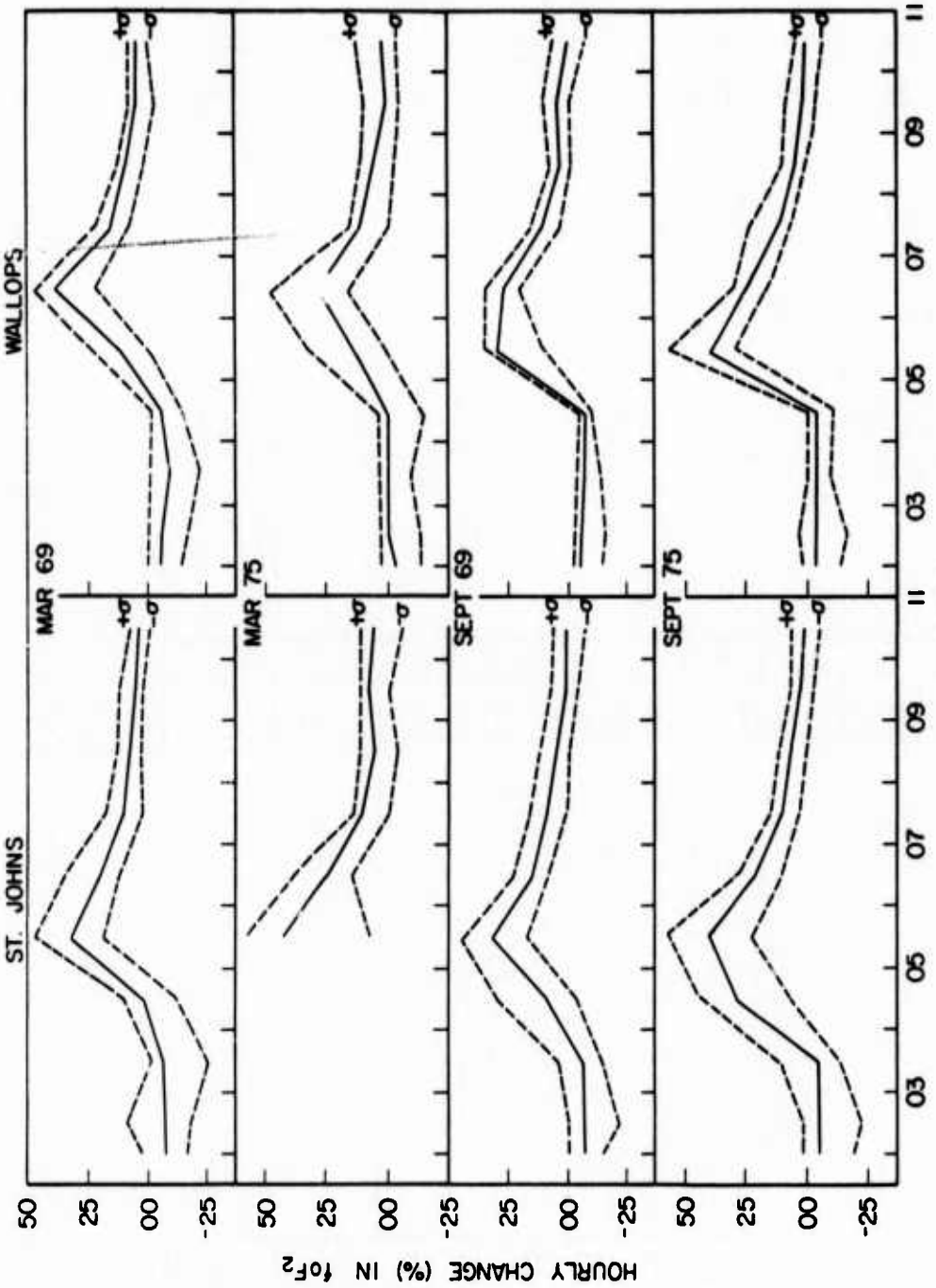

Figure 12a. Percent Hourly Variation of foF2 in the Morning Hours for Equinox

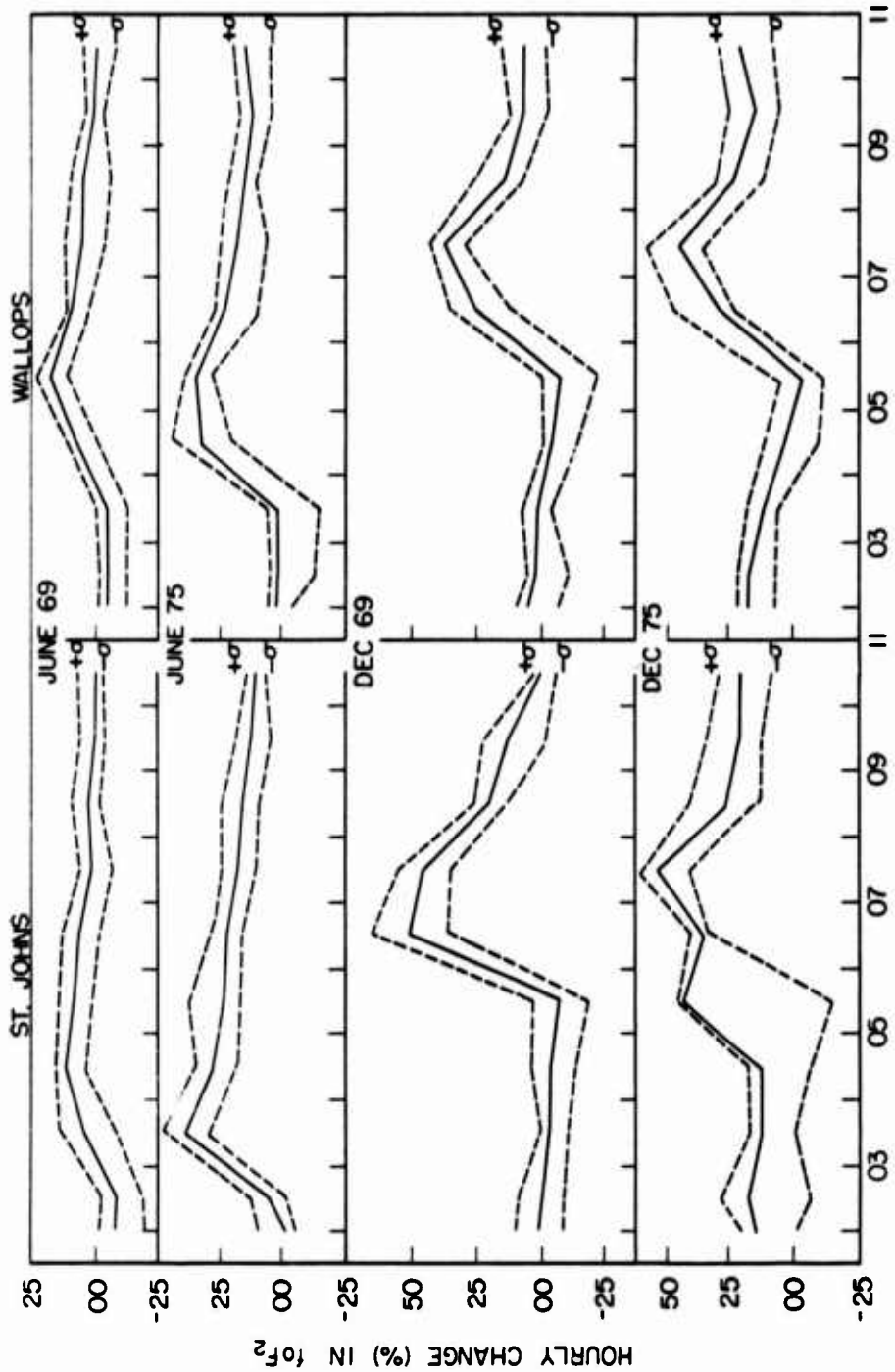

Figure 12b. Percent Hourly Variation of foF2 in the Morning Hours for Solstice

of high (1969) and low (1975) sunspot activity is shown in Figure 9a and for the solstices in Figure 9b. The curves present the median and $\pm\sigma$ values of foF2. A feature common to all the curves is the rapid increase in foF2 during the sunrise period. The effect is largest for the winter month of December and smallest for the summer month of June. The absolute values of foF2 for solar maximum (1969) are twice as large of those for solar minimum (1975). During periods of low solar activity (1975), the foF2 values at the geomagnetically high latitude station St. Johns are routinely 2 MHz or lower, before sunrise. These consistently low foF2s would barely allow the establishment of a barrier at the nominal range of 2000 km (1100 nm) during the late night period, at low solar activity. For all the representative months, there is a rapid increase (large slope) in foF2 for the 2 hours at sunrise followed by a relatively slower increase (smaller slope) for 2 more hours.

The relation

$$P = 100 \times \frac{(foF2_{+\sigma} - foF2_{-\sigma})}{2\ foF2\ Med} \qquad (4)$$

is used to compute the percentage relative variability in foF2 for each hour. Results are shown in Figures 10a and 10b. The curves show that the percent variation does not display any systematic diurnal, seasonal, or solar activity control. The relative day-to-day variability of the hourly data is of the order of 15-20 percent around the median values of foF2. This variability is 2 or 3 times larger than that allowable (~6 percent) to prevent the barrier from moving by more than 250 km (1/2 of its width). Figures 10a and 10b show that, using a fixed (for example, predicted from IONCAP for a given hour) operational frequency, the barrier may start anywhere in a $\pm$750 km distance from the planned 2000 km nominal distance. This 15 percent variability around the hourly median foF2 is superposed on the 20-50 percent hourly change in foF2 during the sunrise transition hours. It is, therefore, essential to reduce this uncertainty through a short term prediction scheme.

For an effective real-time short term prediction, it is necessary to estimate the expected hourly changes in foF2. The hourly slope for the two stations is presented in the same format in Figures 11a and 11b. In addition to median and $\pm\sigma$ levels of the hourly slope of foF2, the lowest slope observed for the month for the particular hour is shown in the figure. The hourly change in foF2 is largest in winter months and smallest in summer months. The change in slope is a factor of 2 larger during the high phase of solar activity than during the low phase of solar activity. The lowest slope is observed to occur on the days of magnetic storms. The highest slope (not shown in the figures) occurs on magnetically quiet days and/or on days corresponding to the recovery from magnetic storms. Even the

curve of lowest slope shows positive magnitude for a few hours at sunrise indicating that the increase in foF2 at sunrise is stronger than the decrease in foF2 associated with magnetic storms.

The relative (percent) hourly slope is computed using the relation

$$\text{Slope} = 200 \times \frac{(foF2_{i+1} - foF2_i)}{(foF2_{i+1} + foF2_i)} . \qquad (5)$$

Plotted in Figures 12a and 12b are the values of the median observed slope and the $\pm\sigma$ level of the slope distribution. The figures show that the relative slope is larger in winter months (December) by almost a factor of 2, as compared with summer and equinox data. But there is no significant difference in relative slope for the respective seasons between high and low solar activity. The relative slope shows a strong diurnal variation. The relative slope reaches its peak 2 hr after sunrise and decreases slowly for the following 2 hr. Thus, the foF2 changes associated with sunrise are significant for a duration of 3-4 hr. The typical peak median slope of 30 percent suggests that the radar frequency has to be adjusted on the average 5 times/hour to accommodate the hourly change in foF2 during the sunrise period.

All the above results can be briefly summarized as: (1) The foF2 noon values as well as the hourly slope of foF2 during sunrise hours are largest in winter and smallest in summer; (2) The relative magnitude (percent increase) of the hourly change in foF2 is twice as large in winter as during equinox and summer; (3) The relative magnitude of the hourly change in foF2 for the particular seasons is reasonably independent of solar cycle activity; (4) The range of foF2 variability at any given hour ($>$ 15-20 percent) is larger than the range acceptable ($<$ 6 percent) for the satisfactory positioning of the barrier; (5) This variation is superposed on the rapid systematic increase in foF2 (of $>$ 30 percent per hour) observed for about 4 hr during the sunrise period, for 6 mo covering the seasons of late fall-winter to early spring.

One of the approaches to improving the prediction of foF2 at one station is to use and extrapolate recent observations from another station to the east of the location of interest. The method can be called the "two station method." For the OTH-B coverage, European stations such as Dourbes (Belgium), Slough (England), or Lindau (Germany) could potentially satisfy the requirements for such predictions at St. Johns in the OTH-B coverage area, provided the two station method works. When one compares the sunrise foF2 slopes over a few hours from two stations like St. Johns and other European stations, one obtains a significant cor-

relation (≥ 0.4), because of the large systematic increase in foF2 due to the sunrise effect at both stations.

Rush and Miller[3] analyzed foF2 data from 32 ionospheric stations to determine the correlation distances for foF2 for the same local time from 1958 data. They found that the correlation distance along the E-W direction is larger than the correlation distance in the N-S direction. They found a diurnal dependence of the correlation distance, with largest correlations at 06 LMT and smallest at 00 LMT. The correlation distance at 06 LMT was 2200 km in the E-W direction and 1500 km in the N-S direction. The separation between European stations Lindau, Slough, or Dourbes and the midpoint sounder at St. Johns is greater than 4000 km. This distance is much larger than the E-W correlation distance of 2200 km beyond which extrapolation becomes unreliable. Davis and Rush[4] analyzed the data for the European stations of OTH-B interest and confirmed the previous findings that on the basis of distance alone, the foF2 observations cannot be extrapolated from European stations to the OTH-B area for obtaining reliable predictions.

For this study, the period of sunrise is determined to last for 5 hr (six hourly observations) consisting of 1-2 hr of pre-sunrise characterized by a flat shape of the foF2 curve followed by 3-4 hr continuous increase in foF2. The foF2 predictions were tested for all data available for these six hourly observations.

In this study, we have investigated the use of real time and recent history of foF2 data from a set of five ionospheric stations (Narssarssuaq, St. Johns, Ottawa, Wallops Island, and Boulder) for the short term prediction (1 hr in advance) of the rapid foF2 changes during sunrise. We considered this approach because, if found useful, it would allow the prediction of the foF2 sunrise transition using the chain of ionospheric sounders deployed for real time ionospheric specification of the ECRS midpoint ionosphere (Goose Bay, St. Johns, Bermuda, Wallops Island).

To judge the performance of the various prediction schemes, we established as a baseline the prediction errors that resulted from the comparison of actual hourly measurements with the predicted foF2 determined from the IONCAP model using the predicted (1 month in advance, not actual) monthly smoothed sunspot number for the respective month.

The proposed prediction scheme uses recent history (for past n days) and real time foF2 observations (day n + 1). Various combinations of IONCAP[2] model predictions and foF2 observations are also tested to determine the best possible prediction to cover the case where no real time data are available due to interruptions in the ionosonde operations.

The proposed scheme is based on the use of the foF2 empirical data base and is shown schematically in Figure 13. The prediction uses averaged foF2 data for four preceding days. As a first-order correction the predicted foF2 is equal to the foF2 now (observed) plus the average foF2 slope for the next hour. As a

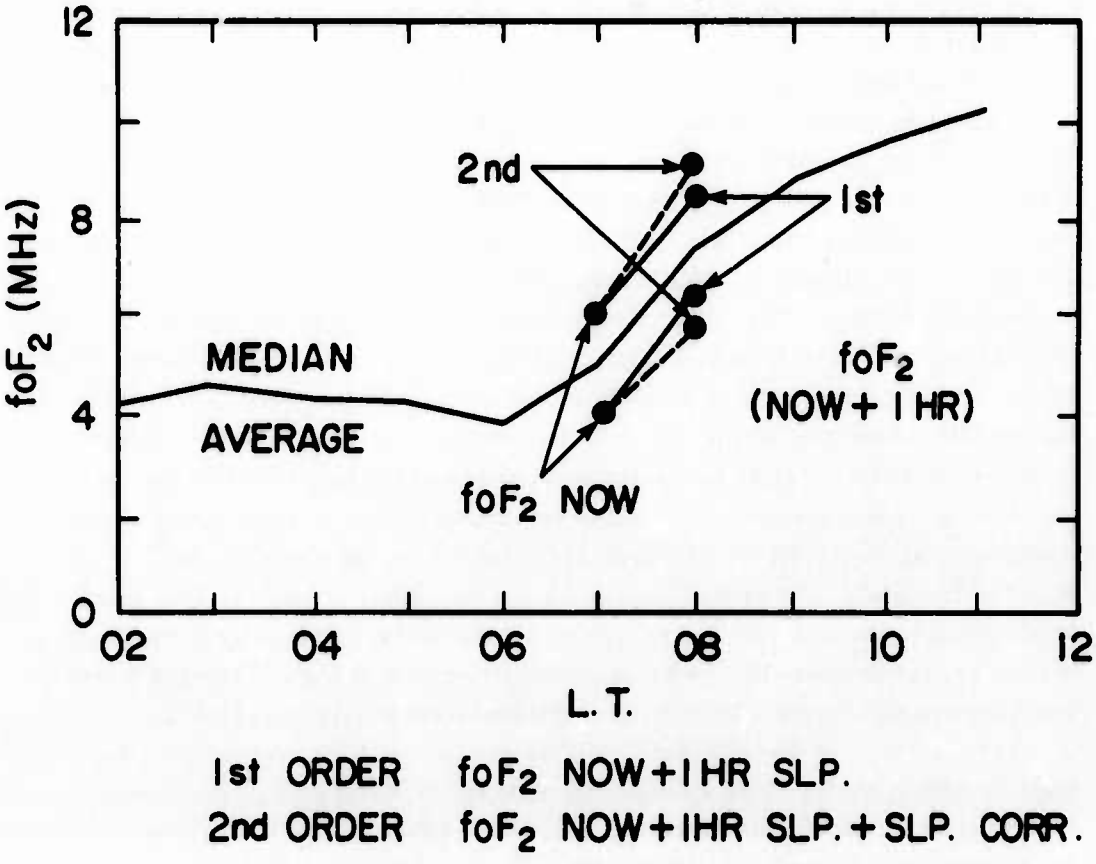

Figure 13. Scheme for Prediction of foF2 at Hourly Intervals From Observed "Now foF2" and Hourly Slope of foF2

second-order correction a slope correction term is made proportional to the difference between foF2 now and the averaged foF2 (for four previous days).

We will first discuss the mathematical procedures used for the various approaches tested and subsequently we will discuss the performance of each scheme.

The prediction for the day n + 1 (prediction day) based on the averaging of samples from n preceding days for the corresponding hour i is given by

$$p(foF2_{n+1,\,i}) = \overline{foF2}_{n,\,i} = \frac{\sum_{1}^{n} foF2_{n,\,i}}{n} \qquad (6)$$

with p(foF2) the predicted foF2 value. Eq. (6) provides averaged foF2 for the past n days as the zeroth order prediction.

If the past days' data is not available, the prediction has to be made using the

IONCAP model, so that the right-hand side of Eq. (6) is simply the foF2 predicted for that hour by the model.

Since real time hourly (or half hourly) foF2 data will be available to the Environmental Assessment (EA) operator at the radar site, we tested the concept of using the actual (i hour) measurement of foF2 in combination with an average slope derived from the prior days' average of foF2 measurements at the i and i + 1 hour to predict foF2 for the i + 1 hour for day n + 1 (prediction day). This scheme is expressed formally as

$$p(foF2_{n+1,\,i+1}) = foF2_{n+1,\,i} + \frac{\sum_{1}^{n} (foF2_{n,\,i+1} - foF2_{n,\,i})}{n} \tag{7}$$

with n + 1 as the day for which the prediction will be made, and n as the number of previous days from which the average foF2 has been determined for the ith hour. In case of lack of the past data, the second term on the right-hand side of Eq. (7) can be replaced by the IONCAP slope.

Finally we added a second order slope correction, which depends on the magnitude of the current foF2 in relation to the past n day average foF2. The prediction is given by:

$$p(foF2_{n+1,\,i+1}) = foF2_{n+1,\,i} + \frac{\sum_{1}^{n} (foF2_{n,\,i+1} - foF2_{n,\,i})}{n} \times \left[1 + \frac{\overline{foF2}_{n,\,i} - foF2_{n+1,\,i}}{\overline{foF2}_{n,\,i}}\right] \tag{8}$$

This means that when the observed foF2 is below the average foF2 of the past n days, the slope correction is larger than the average hourly slope. If foF2 is above the average foF2, the correction is smaller than the average hourly slope. This correction assumes that the tendency is to return towards the median/average curve (value).

Note that the averaged term in the square bracket is same as that in Eq. (6).

In Eqs. (6)-(8), one can use foF2 observations and/or foF2 predictions from the IONCAP model. In general, the analysis shows that the use of recent and real time observations in Eqs. (6)-(8) provides predictions better than those obtained by using foF2s from the IONCAP[2] model.

The method of slopes of foF2 was used for predictions at intervals of 1, 2, and 3 hr respectively. As was expected, the analysis using the 1-hr interval resulted in the smallest errors. Only the results for a 1-hr interval are considered in the following summary. A slope correction similar to Eq. (8) to account for the level of magnetic activity [foF2 slope $\propto (Kp_{n+1} - \overline{Kp})$] was tested. (The WDC Kp index is available at 3-hr intervals only.) The correction was found to be insignificant. Therefore, no such correction was used in the prediction scheme.

The average of prior n days as a prediction was used with values of n = 1, 2, 3, 4, 5, 10, 15, 20, 25. It was determined that for n = 4 the prediction of foF2 yields the least error. Therefore in the following discussion only n = 4 is used.

Eqs. (6), (7), and (8) provide a step by step approach for improving foF2 predictions. The improvement of one prediction scheme over the other is checked in terms of reduction in relative error [see Eq. (9)], reduction in ΔfoF2 [see Eq. (10)], and increase in correlation coefficient showing higher percent of correlated population [see Eq. (12)]. First we will consider the relative error in prediction.

The improvement by a given prediction scheme is determined by comparing errors in prediction at the median (50 percent level), $\pm\sigma$ level and the total range of the data population. For each observation the percent error is determined by

$$\Delta \text{foF2 (\%)} = \frac{\text{foF2}_{obs} - \text{foF2}_{predicted}}{\text{foF2}_{obs}} \qquad (9)$$

The errors are computed from the hourly observations, covering a 6-hr period (2 hr before and 4 hr after sunrise), for each month. From this monthly set of error data, values are determined for median, ± 25 percent, $\pm\sigma$, $\pm 1.5\sigma$, $\pm 2\sigma$ levels and total coverage (extreme values) of the monthly data. In the tables, 3 levels are listed for discussion: median, $\pm\sigma$, and total coverage range.

As an example, the results for Boulder for June 1969 are shown graphically in Figure 14. The figure includes prediction errors to cover ± 25 percent, $\pm\sigma$, $\pm 1.5\sigma$, and $\pm 2\sigma$ levels of the error populations. In the figure for any given level of the populations, the errors are largest for IONCAP predictions and smallest for the proposed method using second-order corrections [see Eq. (8)]. The median error from IONCAP is biased, indicating the inability of IONCAP to predict the median foF2 for the sunrise period, even if the sunspot number is predicted correctly (June 1969, see Table 3). The errors are progressively reduced as one uses the past 4 days' (hourly) averages of foF2, the foF2 now +4 days' average slope, and adding the modified slope [Eq. (8)]. An important aspect of the use of the recent past and the current measurement is that the error distribution is very

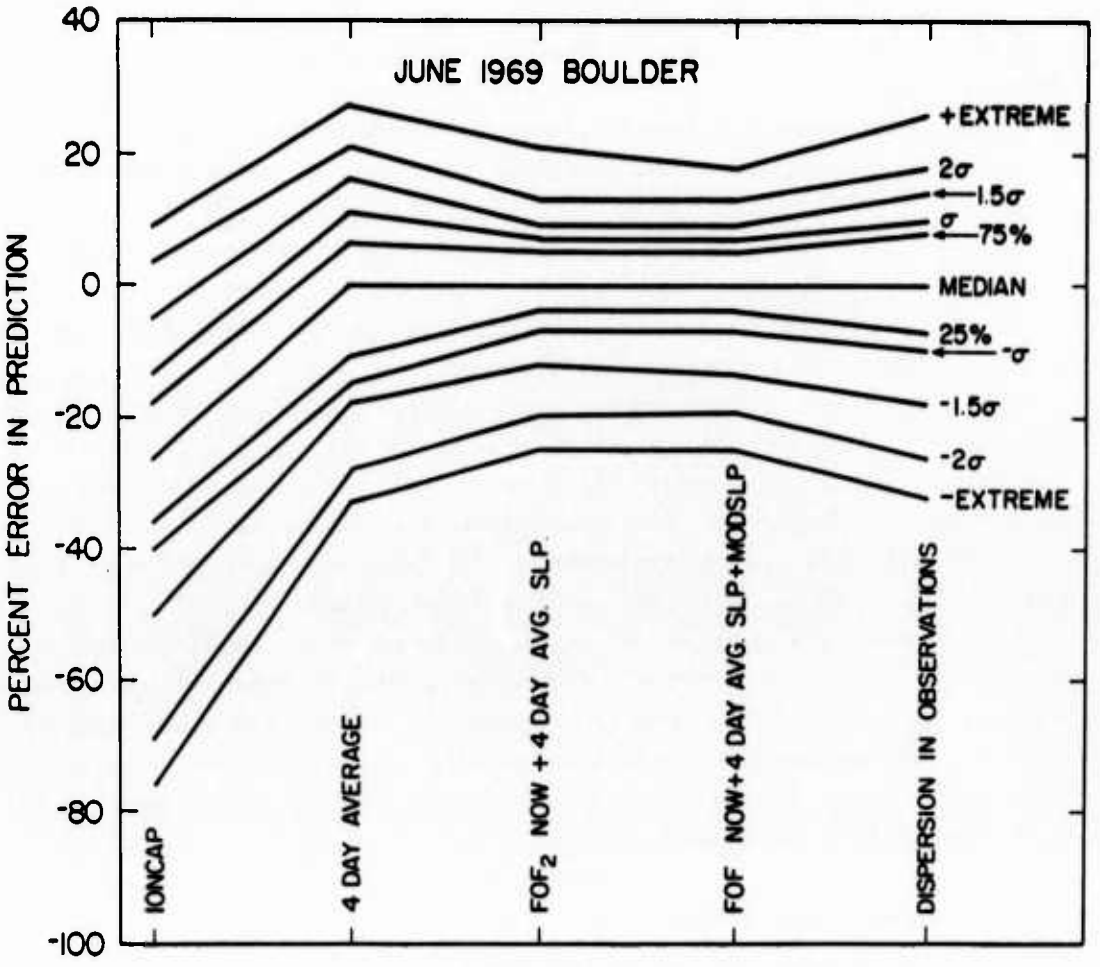

Figure 14. Comparison in the Prediction Error (Percent) of the foF2 for Various Prediction Schemes

nearly centered on zero, that is, in the median over a month, the prediction is close to perfect. Therefore, these approaches make the prediction task independent of specifying or deriving a sunspot number, to drive a prediction model.

The comparison of the percent error of the various methods with the scatter of the data base used around the data median (see last column of Figure 14) is identical to a comparison with the hypothetical case, that IONCAP could predict the monthly median (for the sunrise hours) exactly. The "improvement" of the proposed scheme over the scatter distribution of the data base is also a good estimate of the improvement over the hypothetical case of correct median prediction by IONCAP. The comparison shows that the spread of the observational data around the median is larger than the spread of the errors from the proposed prediction scheme (Figure 14). The figure emphasizes the fact that using the observed

foF2 in Eqs. (6)-(8) yields better predictions than those based on the IONCAP (ITS-78) model.[2]

The results shown in Figure 14 generally repeated in the evaluation of the five station/8 months study. We, therefore, select Eq. (8) as the proposed scheme for improved foF2 prediction during sunrise. In the subsequent discussion of the prediction improvement, we will limit ourselves to the comparison of the errors resulting from the proposed method with those from IONCAP and with the scatter of the data base around the median. This will eliminate the listing of all results showing performance worse than that by Eq. (8).

The results from the analysis are summarized in Table 4. The first column lists the level of the population at which the errors are computed. The second column lists the prediction scheme. The third "method" is essentially the spread in the observed data base. The third column identifies the ionospheric stations providing the data. The next eight columns present the relative (percent) error in prediction for four seasons for high and low sunspot activity periods. The last column presents the average error value for a given station. Looking across the columns, no seasonal dependence is evident, suggesting the extent of data spread (relative) around the median value is independent of seasonal and solar (sunspot) variation. The comparison of average errors from the last column for the prediction schemes shows that errors are significantly smaller for the proposed method at all levels of the distribution.

A reduction in error by the proposed method from those from IONCAP/observed data set is computed by

$$\Delta\text{error} = |\text{ERROR from IONCAP}| - |\text{ERROR from proposed method}| \qquad (10)$$

at respective levels (from Table 4). The results are summarized in Table 5. In the table, a negative sign preceding the value shows that the suggested method caused a deterioration instead of improvement over the method under consideration (blocks with odd sequence number refer to IONCAP, even number to observational data set). A look at the last column shows that the average prediction error is reduced by 8, 8, and 13 percent over IONCAP at the levels of the median, $\pm\sigma$, and total population. In the observed data set, the first term on the right-hand side of Eq. (10) is the spread in data at the respective levels of population. Over the observed data set, the prediction error is reduced by 4 and 7 percent in comparison to the natural spread at $\pm 1\sigma$ and total population, respectively. The result shows that predictions by the proposed scheme are better than the scatter of the observed data (that is, predictions by a perfect IONCAP model).

The percentage reduction in error by the proposed method with respect to IONCAP and the observed data set can be computed by

Table 4. Error (Percent) in foF2 for Various Prediction Methods

At Level	Method	St. No	1969 March	1969 June	1969 September	1969 December	1975 March	1975 June	1975 September	1975 December	Av
Median	IONCAP	1	15	7	5	12	0	6	15	16	9
		2	8	9	5	0	4	6	13	4	6
		3	15	16	9	9	5	6	15	2	9
		4	5	9	6	7	13	13	2	10	8
		5	7	26	21	9	23	37	2	2	16
		Av	10	13	9	7	9	14	9	7	10
	Proposed	1	1	0	2	5	6	0	3	4	3
		2	3	1	0	1	1	1	2	1	1
		3	2	0	1	1	1	0	2	1	1
		4	1	0	1	1	3	2	1	3	2
		5	1	0	0	1	1	3	1	1	1
		Av	2	0	1	2	2	1	2	2	2
	Observed Data Base	1	0	0	2	0	0	0	0	0	0
		2	2	2	3	0	0	0	0	2	1
		3	2	0	1	0	2	0	0	0	1
		4	3	0	0	0	3	0	0	0	1
		5	0	0	0	0	0	0	0	0	0
		Av	1	0	1	0	1	0	0	0	1

1. Narsarssuaq 2. St. Johns 3. Ottawa 4. Wallops 5. Boulder

Table 4 (cont). Error (Percent) in foF2 for Various Prediction Methods

At Level	Method	St. No	1969 March	1969 June	1969 September	1969 December	1975 March	1975 June	1975 September	1975 December	Av
±σ	IONCAP	1	12	12	15	25	38	8	14	15	17
		2	20	14	23	23	13	16	16	13	17
		3	20	17	15	13	18	13	14	14	15
		4	21	12	18	17	21	15	12	18	17
		5	16	27	23	20	25	41	12	18	23
		Av	18	16	19	20	23	19	16	16	18
	Proposed	1	9	9	13	11	9	9	6	14	10
		2	13	8	12	11	8	10	11	12	11
		3	10	7	7	8	11	9	8	11	9
		4	13	6	9	12	7	9	8	11	9
		5	7	7	9	10	9	11	8	9	9
		Av	10	7	10	10	10	9	8	11	10
	Observed Data Base	1	13	13	17	13	18	6	9	10	12
		2	18	16	23	11	13	12	14	11	15
		3	20	14	18	11	17	11	16	11	15
		4	21	13	15	11	18	9	10	9	13
		5	14	10	15	10	14	12	12	14	13
		Av	17	13	18	11	16	10	12	11	13

1. Narsarssuaq 2. St. Johns 3. Ottawa 4. Wallops 5. Boulder

Table 4 (cont). Error (Percent) in foF2 for Various Prediction Methods

At Level	Method	St. No	1969 March	1969 June	1969 September	1969 December	1975 March	1975 June	1975 September	1975 December	Av
Extremes	IONCAP	1	49	27	50	65	60	20	31	68	46
		2	65	40	75	61	31	40	38	40	49
		3	70	26	77	40	50	36	37	36	47
		4	52	37	60	59	70	37	34	47	49
		5	44	43	86	45	60	60	44	64	56
		Av	56	35	70	54	56	39	37	51	49
	Proposed	1	33	23	29	45	28	23	12	33	28
		2	48	53	49	35	24	24	48	50	41
		3	50	18	51	38	96	19	27	35	42
		4	34	41	36	31	18	31	33	58	35
		5	37	21	32	29	58	35	29	45	36
		Av	40	31	39	36	45	26	30	44	36
	Observed Data Base	1	55	28	49	50	50	16	36	45	41
		2	68	39	75	38	37	26	31	30	43
		3	85	33	86	35	48	30	33	45	49
		4	60	41	47	35	36	32	32	29	39
		5	45	29	60	37	47	36	44	42	42
		Av	63	34	63	39	44	28	35	38	43

1. Narsarssuaq 2. St. Johns 3. Ottawa 4. Wallops 5. Boulder

Table 5. Error Reduction (Percent) by Proposed Method Over Other Methods

At Level	Method	St. No	1969 March	1969 June	1969 September	1969 December	1975 March	1975 June	1975 September	1975 December	Av
Median	IONCAP	1	14	7	2	7	-6	6	12	12	7
		2	5	8	5	-1	3	5	10	3	5
		3	14	16	8	1	4	6	13	1	8
		4	4	9	5	5	10	11	1	7	7
		5	6	26	20	8	22	34	1	1	15
		Av	10	13	8	4	6	12	7	5	8
	Observed Data Base	1	-1	0	0	-5	-6	0	-3	-4	-2
		2	-1	1	3	-1	-1	-1	-2	1	0
		3	0	0	1	-1	1	0	-2	-1	0
		4	2	0	-1	-1	0	-2	-1	-3	-1
		5	1	0	0	-1	-1	-3	-1	-1	-1
		Av	0	0	0	-1	-1	-1	-2	-2	-1
±σ	IONCAP	1	3	3	2	14	29	-2	8	1	7
		2	8	6	11	12	5	6	5	1	7
		3	10	10	8	4	4	4	5	3	7
		4	8	6	9	5	14	7	4	7	8
		5	8	20	13	10	16	30	4	9	14
		Av	7	9	8	9	14	9	5	4	8
	Observed Data Base	1	4	4	4	1	9	-3	3	-4	2
		2	6	8	11	1	5	1	2	-1	4
		3	9	7	11	3	5	2	7	0	6
		4	8	7	6	-1	11	0	2	-1	4
		5	7	3	5	0	5	1	4	5	4
		Av	7	6	7	1	7	0	4	0	4

1. Narsarssuaq 2. St. Johns 3. Ottawa 4. Wallops 5. Boulder

Table 5 (cont). Error Reduction (Percent) by Proposed Method Over Other Methods

At Level	Method	St. No	1969 March	1969 June	1969 September	1969 December	1975 March	1975 June	1975 September	1975 December	Av
Extremes	IONCAP	1	16	4	21	20	32	-3	20	34	18
		2	17	-12	26	27	7	17	-10	-10	8
		3	20	7	26	2	-46	16	10	1	5
		4	17	-3	25	28	52	6	1	-11	14
		5	7	22	54	16	2	25	15	19	20
		Av	15	5	30	19	9	12	7	7	13
	Observed Data Base	1	21	5	19	5	22	-7	24	11	13
		2	20	-14	26	3	13	3	-17	-20	2
		3	35	15	35	-2	-48	11	6	9	7
		4	26	0	11	4	13	1	0	-30	4
		5	7	9	28	8	-11	1	15	-2	7
		Av	22	3	24	4	-1	2	6	-6	7

1. Narsarssuaq 2. St. Johns 3. Ottawa 4. Wallops 5. Boulder

$$\text{factor (percent)} = 100 \times \frac{(\Delta\text{ERROR}_i - \Delta\text{ERROR}_{\text{PROPOSED METHOD}})}{\text{ERROR}_i} \qquad (11)$$

where i - refers to values from IONCAP and from observational data set respectively. The term ΔERROR is the spread in the observational data base.

The improvement factors are computed by use of respective values from Table 4. The results from the last columns of Tables 4 and 5 and evaluation by Eq. (11) are summarized in Table 6. The table is divided into three major sections. These list error, reduction in error and improvement respectively. Each column is subdivided in three columns to present the median, ±1σ and total population coverage. Each block (along the row) refers to a prediction method. The line at the bottom of each block presents the average value from all the stations. Referring to lines in the last three columns, the proposed method shows 86 percent improvement (factor) in prediction over that from IONCAP. Such a large improvement is due to a reduction in bias in the IONCAP prediction seen in Figure 14. At the ±1σ level, the proposed method provides an improvement (factor) of 47 percent over IONCAP and of 29 percent over the observed data set. The overall (total population) improvement (factor) is 26 percent over IONCAP and of 16 percent over the observed data set.

One may choose the reduction in ΔfoF2 instead of that relative to foF2 (as presented in Tables 4 to 6). The results are presented in Tables 7 to 9 respectively, using the same format as for Tables 4 to 6.

A look at the first block of Table 9, presenting the summary of the results, shows that, on the average, IONCAP predictions are off by ±0.4, ±0.7, and ±1.7 MHz at median, ±1σ and total population levels. The improvement by the suggested method over IONCAP reduces the error at these levels by 0.4 MHz. The last block shows that the prediction by the new method reduces the error compared to the spread in the natural data base by 0.2 MHz at the ±1σ level and by 0.3 MHz in the overall data base.

The second block shows that the new method reduces the prediction error to ±0.4 MHz at the ±σ level population satisfying the prediction requirement of ±0.5 MHz suggested for the East and West Coast radar operations.

The tables show that the method proposed here will provide better predictions than IONCAP, and also a lesser scatter in prediction errors than those existing in the natural data base (that is, improved prediction over that from a perfect IONCAP).

The analysis of the various prediction schemes was extended to restrict prediction to quiet days only. The data of the five most disturbed days in each month were excluded from the analysis, and no predictions were computed for the dis-

Table 6. Summary of Error, Reduction in Error and Improvement by Proposed Method

Method	St. No	Percent Error at			Percent Error Reduction by Proposed Method at			Improvement Factor Percent by Proposed Method at		
		Median	±σ Level	Extremes	Median	±σ Level	Extremes	Median	±σ Level	Extremes
IONCAP	1	9	17	46	7	7	18	78	41	39
	2	6	17	49	5	7	8	83	41	16
	3	9	15	47	8	7	5	89	47	11
	4	8	17	49	7	8	14	88	47	29
	5	16	23	56	15	14	20	94	61	36
	Av	10	18	49	8	8	13	86	47	26
Proposed	1	3	10	28						
	2	1	11	41						
	3	1	9	42	← N/A →			← N/A →		
	4	2	9	35						
	5	1	9	36						
	Av	1	10	36						
Observa-tional Data Base	1	0	12	41		2	13		17	32
	2	1	15	43		4	2		27	5
	3	1	15	49		6	7		40	14
	4	1	13	39		4	4		31	10
	5	0	13	42		4	7		31	17
	Av	1	13	43		4	6		29	16

1. Narsarssuaq 2. St. Johns 3. Ottawa 4. Wallops 5. Boulder N/A - Not Applicable

Table 7. ΔfoF2 Errors in Predictions From Various Methods

At Level	Method	St. No	1969 March	1969 June	1969 September	1969 December	1975 March	1975 June	1975 September	1975 December	Av
Median	IONCAP	1	0.7	0.4	0.2	0.6	0	0.2	0.5	0.4	0.4
		2	0.4	0.5	0.3	0	0.1	0.2	0.4	0.2	0.3
		3	1.0	0.9	0.4	0.1	0.2	0.2	0.6	0.1	0.4
		4	0.2	0.4	0.2	0.4	0.4	0.4	0.1	0.4	0.3
		5	0.4	1.3	1.0	0.6	0.7	1.2	0.1	0.1	0.7
	Proposed	1	0	0	0.1	0.2	0.2	0	0.1	0.1	0.1
		2	0.1	0	0	0.1	0	0	0.1	0	0
		3	0.1	0	0	0.1	0	0	0.1	0	0
		4	0	0	0	0.1	0.1	0.1	0	0.1	0.1
		5	0.1	0	0	0.1	0	0.1	0	0	0
	Observed Data Base	1	0	0	0.1	0	0	0	0	0	0
		2	0.1	0.1	0.2	0	0	0	0	0.1	0.1
		3	0.1	0	0.1	0	0.1	0	0	0	0
		4	0.1	0	0	0	0.1	0	0	0	0
		5	0	0	0	0	0	0	0	0	0

1. Narsarssuaq 2. St. Johns 3. Ottawa 4. Wallops 5. Boulder

Table 7 (cont). ΔfoF2 Errors in Predictions From Various Methods

At Level	Method	St. No	1969 March	1969 June	1969 September	1969 December	1975 March	1975 June	1975 September	1975 December	Av
±σ	IONCAP	1	0.7	0.7	0.8	0.9	0.6	0.3	0.5	0.4	0.6
		2	1.0	0.9	1.1	1.1	0.4	0.5	0.6	0.6	0.8
		3	1.3	1.0	1.0	0.8	0.6	0.5	0.6	0.7	0.8
		4	1.1	0.6	0.7	0.6	0.6	0.4	0.4	0.5	0.6
		5	0.8	1.3	1.0	0.9	0.8	1.2	0.5	0.7	0.9
	Proposed	1	0.5	0.5	0.5	0.5	0.2	0.4	0.3	0.4	0.4
		2	0.6	0.4	0.5	0.5	0.3	0.3	0.3	0.5	0.4
		3	0.6	0.3	0.4	0.5	0.4	0.3	0.3	0.5	0.4
		4	0.7	0.3	0.4	0.5	0.3	0.2	0.3	0.4	0.4
		5	0.4	0.4	0.5	0.5	0.3	0.3	0.3	0.4	0.4
	Observed Data Base	1	0.7	0.6	0.8	0.5	0.5	0.2	0.3	0.3	0.5
		2	0.8	0.8	1.0	0.6	0.4	0.3	0.4	0.4	0.6
		3	1.3	0.7	1.0	0.7	0.6	0.4	0.5	0.6	0.7
		4	1.0	0.6	0.7	0.6	0.5	0.3	0.3	0.4	0.5
		5	0.7	0.6	0.7	0.6	0.4	0.4	0.5	0.6	0.6

1. Narsarssuaq 2. St. Johns 3. Ottawa 4. Wallops 5. Boulder

Table 7 (cont). ΔfoF2 Errors in Predictions From Various Methods

At Level	Method	St. No	1969 March	1969 June	1969 September	1969 December	1975 March	1975 June	1975 September	1975 December	Av
Extremes	IONCAP	1	2.2	1.3	2.2	2.3	1.0	0.6	0.9	1.6	1.5
		2	3.3	1.9	2.7	2.5	1.0	0.9	1.6	1.3	1.9
		3	3.7	1.6	2.6	2.2	1.4	1.0	1.5	1.5	1.9
		4	3.0	1.6	1.7	1.8	0.9	0.8	1.3	1.2	1.5
		5	2.7	1.7	2.9	2.6	1.5	1.1	1.5	1.8	1.9
	Proposed	1	1.4	1.0	1.1	1.3	0.5	0.7	0.5	1.1	1.0
		2	1.7	1.9	1.1	2.6	0.8	0.8	1.2	1.4	1.4
		3	1.8	1.0	2.1	1.7	2.2	0.8	1.0	1.6	1.5
		4	1.7	1.3	1.3	2.2	0.7	0.7	0.8	1.2	1.2
		5	1.8	1.0	1.9	2.2	1.5	0.9	1.0	1.3	1.4
	Observed Data Base	1	2.2	1.3	2.2	1.7	0.9	0.6	0.8	1.4	1.4
		2	3.1	1.8	2.7	2.3	0.9	0.8	1.4	1.3	1.8
		3	3.7	1.7	2.4	1.8	1.1	0.9	1.5	1.6	1.8
		4	3.0	1.5	1.7	1.4	0.8	0.7	1.3	1.0	1.4
		5	2.6	1.5	2.9	2.1	1.4	0.9	1.5	1.4	1.8

1. Narsarssuaq 2. St. Johns 3. Ottawa 4. Wallops 5. Boulder

Table 8. Reduction in ΔfoF2 (MHz) by Proposed Method Over Other Methods

At Level	Method	St. No	1969 March	1969 June	1969 September	1969 December	1975 March	1975 June	1975 September	1975 December	Av
Median	IONCAP	1	0.7	0.4	0.1	0.4	-0.2	0.2	0.4	0.3	0.3
		2	0.3	0.5	0.3	-0.1	0.1	0.2	0.3	0.2	0.2
		3	0.9	0.9	0.4	0	0.2	0.2	0.5	0.1	0.4
		4	0.2	0.4	0.2	0.3	0.3	0.3	0	0.3	0.2
		5	0.3	1.3	1.0	0.5	0.7	1.1	0.1	0.1	0.6
		Av	0.5	0.7	0.5	0.2	0.2	0.4	0.3	0.2	0.3
	Observed Data Base	1	0	0	0	-0.2	-0.2	0	-0.1	-0.1	0.1
		2	0	0.1	0.2	-0.1	0	0	-0.1	-0.1	0
		3	0	0	0.1	-0.1	0.1	0	-0.1	0	0
		4	0.1	0	0	-0.1	0	-0.1	0	-0.1	0
		5	-0.1	0	0	-0.1	0	-0.1	0	0	0
		Av	0	0	0.1	-0.1	0	0	-0.1	-0.1	0
±σ	IONCAP	1	0.1	0.2	0.3	0.4	0.3	-0.1	0.3	-0.1	0.2
		2	0.4	0.5	0.5	0.6	0.1	0.2	0.3	0	0.3
		3	0.6	0.7	0.6	0.3	0.2	0.1	0.2	0.2	0.4
		4	0.4	0.3	0.3	0.1	0.3	0.2	0.1	0.1	0.2
		5	0.4	0.9	0.5	0.4	0.5	0.8	0.2	0.3	0.5
		Av	0.4	0.5	0.4	0.4	0.5	0.2	0.2	0.1	0.3
	Observed Data Base	1	0.1	0.1	0.3	0	0.3	0.2	0	-0.2	0.1
		2	0.1	0.4	0.5	0.1	0.1	0	0.1	-0.1	0.1
		3	0.7	0.4	0.6	0.2	0.2	0.1	0.1	0	0.3
		4	0.3	0.3	0.2	0	0.2	0.1	0	0	0.1
		5	0.3	0.2	0.2	0.1	0.2	0.1	0.2	0.2	0.2
		Av	0.3	0.3	0.4	0.1	0.2	0.1	0.1	0	0.2

1. Narsarssauq 2. St. Johns 3. Ottawa 4. Wallops 5. Boulder

Table 8 (cont). Reduction in ΔfoF2 (MHz) by Proposed Method Over Other Methods

At Level	Method	St. No	1969 March	1969 June	1969 September	1969 December	1975 March	1975 June	1975 September	1975 December	Av
Extremes	IONCAP	1	0.8	0.3	1.0	1.0	0.5	-0.1	0.4	0.5	0.5
		2	1.5	[illegible]	1.6	-0.1	0.2	0.1	0.4	-0.1	0.5
		3	1.9	0.6	0.5	0.4	-0.8	0.2	0.5	-0.2	0.4
		4	1.3	0.3	0.4	-0.4	0.2	0	0.4	-0.1	0.3
		5	0.9	0.6	1.0	0.3	0	0.2	0.5	0.4	0.5
		Av	1.3	0.4	0.9	0.2	0	0.1	0.4	0.1	0.4
	Observed Data Base	1	0.8	0.3	1.0	0.3	0.4	-0.1	0.3	0.2	0.4
		2	1.4	-0.1	1.6	-0.3	0.2	0	0.2	-0.2	0.3
		3	1.9	0.6	0.3	0	-1.1	0.1	0.5	-0.1	0.3
		4	1.3	0.1	0.4	-0.8	0.1	0	0.4	-0.2	0.2
		5	0.7	0.4	1.0	-0.1	-0.1	0	0.5	0	0.3
		Av	1.2	0.3	0.9	-0.2	-0.1	0	0.4	-0.1	0.3

1. Narsarssauq 2. St. Johns 3. Ottawa 4. Wallops 5. Boulder

Table 9. Summary of ΔfoF2 (MHz) Error and Reduction in Error (ΔfoF2) by Proposed Method

Method	St. No	Δ foF2 MHz at Level			ΔfoF2 MHz (Reduction) at Level		
		Median	±σ	Extremes	Median	±σ	Extremes
IONCAP	1	0.4	0.6	1.5	0.3	0.2	0.5
	2	0.3	0.8	1.9	0.2	0.3	0.5
	3	0.4	0.8	1.9	0.4	0.4	0.4
	4	0.3	0.6	1.5	0.2	0.2	0.3
	5	0.7	0.9	1.9	0.6	0.5	0.5
	Av	0.4	0.7	1.7	0.4	0.3	0.4
Proposed	1	0.1	0.4	1.0			
	2	0	0.4	1.4			
	3	0	0.4	1.5			
	4	0.1	0.4	1.2			
	5	0	0.4	1.4			
	Av	0.1	0.4	1.3			
Observed Data Set	1	0	0.5	1.4		0.1	0.4
	2	0.1	0.6	1.8		0.1	0.3
	3	0	0.7	1.8		0.3	0.3
	4	0	0.5	1.4		0.1	0.2
	5	0	0.6	1.8		0.2	0.3
	Av	0	0.6	1.5		0.2	0.3

1. Narsarssuaq 2. St. Johns 3. Ottawa 4. Wallops 5. Boulder

turbed days' foF2s. The results are slightly better but not significantly different from those presented in Tables 4 to 9.

In the above discussion, we considered relative (percent) and magnitude improvements in foF2, obtained by the proposed method over the IONCAP method and over the observational data set.

The degree of improvement equation used by Davis and Rush[4] deals with the fractions of correlated and uncorrelated populations of the data set. The equation (Gautier and Zacharisen[9]) is

---

9. Gautier, T.N., and Zacharisen, D.H. (1965) Use of space and time correlations in short term ionospheric predictions, Conference Record 1st Annual IEEE Communications Convention, pp. 671-676.

$$I = 100\ [1 - (1 - R^2)^{1/2}] \qquad (12)$$

where I is the degree of improvement in percent and R is the correlation coefficient.

First let us delete the multiplying factor 100 so that R and I become comparable quantities with ranges from -1 to + 1. Further replacing I by 1 - I', we obtain $R^2 + I'^2 = 1$ where the partition of the correlated and uncorrelated fractions of the data set is clearly evident.

The distributions of these correlated and uncorrelated populations for the two prediction schemes: (1) IONCAP, (2) Proposed Method, and for the use of the scatter of the observed data around the monthly median foF2 (perfect IONCAP) are computed. The least squared deviation with first order (linear) fit is computed among foF2s predicted by the proposed method vs the observed hourly foF2 data set. The correlation coefficients are summarized in Table 10, which has the same format as that for Table 9. The third column presents the values for the correlation coefficients. The range of percent population correlated is given by R^2 to R as listed in the next column. The table shows that the correlation coefficients for the proposed method are highest compared to those from the IONCAP and the observed median foF2s. The degree of improvement computed by the use of Eq. (7) is in the following column. These again confirm that the proposed method offers an improvement. The improvement (ΔI) achieved by proposed method over IONCAP and the observed data distribution (perfect IONCAP) is presented in column 6. The results show that additional 14 and 10 percent populations are shifted from the non-correlated group to the correlated group, for IONCAP and observed median foF2 prediction methods. The last column shows relative improvement [similar to Eq. (11)]. Thus the proposed method offers a relative improvement of 29 and 20 percent over the respective methods. The transmitter site is 1100-1340 km from the mid-point region of OTH-B interest. Though the correlation distance is just about right, the two station method is unable to predict hourly foF2 at St. Johns for the sunrise transition period from the larger and leading changes in foF2 observed at the European stations.

5. CONCLUSIONS

The analysis of data from five stations representing the OTH-B coverage area has been conducted for four seasons of two selected years to cover high and low phases of solar cycle activity.

Between two prediction schemes: (1) use of data from a single station, and (2) extrapolation of data from one station to another, the first is better. For a

Table 10. Comparisons of Correlations and Improvements Among Prediction Schemes Used

Method	St. No	Corr. Coeff R	Range R^2 to R	Degree of Improvement (I)	Improvement by Proposed Method (ΔI)	Relative Improvement (Percent) by Proposed Method
IONCAP	1	0.79	62 - 79	0.42	0.08	19
	2	0.82	67 - 82	0.47	0.15	32
	3	0.82	67 - 82	0.46	0.17	37
	4	0.89	79 - 89	0.57	0.13	23
	5	0.86	74 - 86	0.49	0.17	35
	Av	0.84	71 - 84	0.48	0.14	29
Proposed	1	0.85	72 - 85	0.50		
	2	0.92	85 - 92	0.62		
	3	0.93	86 - 93	0.64		
	4	0.95	90 - 95	0.70		
	5	0.94	79 - 94	0.66		
	Av	0.92	85 - 92	0.62		
Observed Data Set	1	0.82	67 - 82	0.47	0.03	6
	2	0.86	74 - 86	0.53	0.09	17
	3	0.84	71 - 84	0.49	0.15	31
	4	0.90	81 - 90	0.60	0.10	17
	5	0.87	76 - 87	0.52	0.14	27
	Av	0.86	74 - 86	0.52	0.10	20

1. Narsarssuaq 2. St. Johns 3. Ottawa 4. Wallops 5. Boulder

given station, out of various alternatives, such as the use of observed median foF2, IONCAP predictions using the predicted sunspot number, and averaging the data for "n" number of days prior to the prediction day, the four-day averages is the best approach. The prediction is further improved by application of first- and second-order slope correction shown by Eqs. (7) and (8). The predictions are very slightly improved if magnetically disturbed days are neglected in the prediction scheme. An important feature of the proposed scheme is that the prediction error distribution has a negligible median error. The scheme makes short term predictions independent of the still imprecise prediction of the relevant sunspot numbers.

In summary, the steps in the prediction of foF2 during the sunrise period are as follows: (1) For each LT hour of the sunrise period, store the hourly foF2s from observations of up to 4 days prior to prediction. Exclude the days that are found to be magnetically severely disturbed. (2) Determine the hourly slope of foF2 for each day and average up to four slopes. (3) To the current foF2 observation, add the relevant mean hourly slope, add a correction term of slope [Eq. (8)] that is a function of deviation of $foF2_{now}$ from the (4 day) averaged foF2. This provides, from the schemes tested, the best prediction for the foF2 at the next hour.

The deployment of digital ionosondes with automatic data processing capabilities (Reinisch et al[6]) will make real time half hourly data available to the EA operators. We plan to analyze the proposed scheme for use of half hourly real time data, which should improve the predictions even further. A real time test using Goose Bay and Argentia data will be initiated in the near future. A further improvement in prediction of the radar frequencies to be used requires the incorporation of the change in layer height during sunrise into the prediction scheme. We are currently investigating available data bases as to their usefulness for this analysis.

REFERENCES

1. Barghausen, A.L., Finney, J.W., Proctor, L.L., and Schultz, L.D. (1969) Predicting Long Term Operational Parameters of High Frequency Sky-Wave Telecommunications Systems, ESSA Technical Report ERL 110-ITS78.

2. Lloyd, J.L., Haydon, G.W., Lucas, D.L., and Teters, L.R. (1978) Estimating the Performance of Telecommunication Systems Using the Ionospheric Transmission Channel, National Telecommunications and Information Administration, Boulder, Colo.

3. Rush, C.M., and Miller, D. (1973) A Three-Dimensional Ionospheric Model Using Observed Ionospheric Parameters, AFCRL-TR-73-0567, AD 772672.

4. Davis, R.M., Jr., and Rush, C.M. (1983) Feasibility of Forecasting foF2 Disturbances During the Sunrise Transition Period, Technical Memorandum Series NTIA-TM-83-87, U.S. Department of Commerce, National Telecommunications and Information Administration.

5. Appleton, E.V., and Beynon, W.J.G. (1940) The application of ionospheric data to radio communication problems, Part I., Proc. Phys. Soc., Part I, 52:518.

6. Reinisch, B.W., Gamache, R.R., Tang, J.S., and Kitrosser, D.F. (1983) Automatic Real Time Ionogram Scaler With True Height Analysis - ARTIST, AFGL-TR-83-0209, AD A135174.

7. Buchau, J., Weber, E.J., Anderson, D.N., Carlson, H.C., Jr., and Moore, J.G. (1985) Ionospheric structures in the polar cap, their relation to satellite scintillations, in the Effect of the Ionosphere on C^3I Systems Symposium Proceedings of Ionospheric Effects Symposium, J.M. Goodman, Ed.

8. Mendillo, M., Lynch, F.X., and Klobuchar, J.A. (1980) Geomagnetic activity control of ionospheric variability, in Prediction of Terrestrial Effects of Solar Activity, Vol. 4 of Solar-Terrestrial Predictions Proceedings, R.F. Donnelly, Ed., Space Environment Laboratory, National Oceanic and Atmospheric Administration, Boulder, Colo.

9. Gautier, T.N., and Zacharisen, D.H. (1965) Use of space and time correlations in short term ionospheric predictions, Conference Record 1st Annual IEEE Communications Convention, pp. 671-676.